Title

APPARATUS FOR HEAT CAPACITY MEASUREMENTS IN THE RANGE 0.24 TO 20|K; APPLICATIONS TO SOME TRANSITION-METAL SUPERCONDUCTORS AND FERRCMAGNETIC-SUPERCONDUCTORS

Author

Batt, Russell Howard.

Publication Date

1964-09-01

Thesis/dissertation

UCRL-11580

University of California

Ernest O. Lawrence Radiation Laboratory

APPARATUS FOR HEAT CAPACITY MEASUREMENTS IN THE RANGE 0.24 TO 20°K; APPLICATIONS TO SOME TRANSITION-METAL SUPERCONDUCTORS AND FERROMAGNETIC-SUPERCONDUCTORS

Berkeley, California

DISCLAIMER

UCRL-11580

UNIVERSITY OF CALIFORNIA

Lawrence Radiation Laboratory
Berkeley, California

AEC Contract No. W-7405-eng-48

APPARATUS FOR HEAT CAPACITY MEASUREMENTS IN THE RANGE 0.24 to 20°K; APPLICATIONS TO SOME TRANSITION-METAL SUPERCONDUCTORS AND FERROMAGNETIC-SUPERCONDUCTORS

Russell Howard Batt

(Ph.D. Thesis)

September 1964

APPARATUS FOR HEAT CAPACITY MEASUREMENTS IN THE RANGE 0.24 TO 20°K; APPLICATIONS TO SOME TRANSITION-METAL SUPERCONDUCTORS AND FERROMAGNETIC-SUPERCONDUCTORS

CONTENTS

APPARATUS FOR HEAT CAPACITY MEASUREMENTS IN THE RANGE 0.24 TO 20°K; APPLICATIONS TO SOME TRANSITION-METAL SUPERCONDUCTORS AND FERROMAGNETIC-SUPERCONDUCTORS

Russell Howard Batt

Inorganic Materials Research Division, Lawrence Radiation Laboratory,
Department of Chemistry, College of Chemistry,
University of California, Berkeley, California

ABSTRACT

An apparatus for heat capacity measurements in the temperature range 0.24 to 20°K, using liquid ^3He, ^4He or H_2 as cooling agents, is described. The main components of the low temperature part of the apparatus are a copper block which contains a vapor pressure bulb and a chamber into which ^3He is condensed, a magnetic thermometer for measuring temperatures below 1°K, and two mechanical heat switches to provide thermal contact between the sample and the copper block and between the block and the liquid ^4He or H_2 bath. The temperature of the copper block can be maintained constant to 0.01% at most temperatures within the range 0.24 to 20°K.

The heat capacity of ruthenium was measured from 0.27 to 1.2°K. Several parameters characteristic of the superconducting state are derived from the heat capacity measurements and are compared with those of several other superconductors. This comparison shows no obvious difference to exist between ruthenium and those superconductors which exhibit the isotope effect. A correlation is found to exist between the deviations of these parameters from the BCS values and T_c/θ_o, indicating that the main features of the critical field curve conform to a law of corresponding states which includes the additional parameter T_c/θ_o. Ruthenium is shown to fit into this correlation.

The heat capacities of Ti, and of Ti containing 0.05%, 0.25% and 1.0% Fe were measured from 0.24 to 4.2°K. The results show the absence of an ordinary bulk superconducting transition in all of the samples. A reduced superconducting transition is observed in the 1% Fe-Ti alloy at ≈ 3°K, in agreement with magnetic measurements, but a large linear term in the heat capacity at temperatures below this transition suggests either that the superconductivity is not of the usual kind or that only 15% of the sample participates in the superconducting transition. The present results are compared with related work on Mn-Ti alloys.

Heat capacity measurements were made from 0.25 to 20°K on two solid solutions ($Y_{1-x}Gd_xOs_2$) in which superconductivity and ferromagnetic ordering were found by magnetic measurements to coexist. The present results, together with some earlier heat capacity measurements, indicate that the magnetic and superconducting ordering occur together in the same volume elements of the sample.

I. APPARATUS

A. General Description

Until recently, most heat capacity measurements at temperatures below the triple point of hydrogen have been confined to the temperature range 1.2 to 4.2°K, which is easily accessible with liquid ^{4}He. In the past few years, adiabatic demagnetization of a paramagnetic salt has been used to extend the range of heat capacity measurements to below 0.1°K, and ^{3}He cryostats have been used between 0.3 and 1.2°K. There are many cases in which heat capacity measurements from below 1°K to above 20°K would be of considerable interest, but with most of the calorimeters that have been used previously, measurements over such an extended temperature range would require two or three separate experiments.

The apparatus to be described here is designed so that measurements can be made from 0.25 to above 20°K in a single experiment. The requirements for making heat capacity measurements at ^{3}He temperatures and between 4.2 and 14°K are sufficiently similar that it is practical to design a calorimeter which will work in each of these temperature ranges and in the liquid ^{4}He and liquid H_2 ranges as well. The requirements for a calorimeter using adiabatic demagnetization are, however, sufficiently different that it was decided to be impractical to extend the range of the present apparatus below 0.25°K. The different nature of the experimental problems encountered below 0.25°K and above 20°K suggests these temperatures as natural points at which to change to different types of calorimeters.

Figure 1 shows, in schematic cross section, the low temperature part of the cryostat used in these experiments. The copper block, which

was machined from a single piece of high purity copper, contains a chamber into which the ^3He is condensed, a vapor pressure bulb, and several small clamps for mounting a platinum resistance thermometer and germanium resistance thermometers. Attached to the bottom of the block is a copper cage in which the sample is rigidly suspended by means of cotton threads. A cerium magnesium nitrate crystal, used to measure temperatures below 1°K, is rigidly attached to the bottom of the cage by means of a Plexiglas clamp. The salt crystal is thermally connected to the sample cage which, in turn, is thermally connected to the block. The block and cage assembly is thermally isolated from the surrounding liquid ^4He (or liquid H_2) bath by a vacuum can.

Thermal contact between the copper block and the surrounding bath, and between the copper block and the sample is provided by two mechanical heat switches, hereafter referred to as the upper and lower switches, respectively. Each switch is actuated by a 0.025 inch diameter stainless steel wire, the room temperature end of which is attached to a vertical-motion screw mechanism. At several widely spaced points, each stainless steel wire is thermally anchored to the ^4He bath to minimize heat conduction along the wire to the block. The jaws of each mechanical heat switch are thermally connected directly to the block or to the bath by means of heavy, flexible copper wires. The thermal resistance of the lower (sample to block) heat switch was measured by determining the equilibrium temperature difference existing between the sample and the block produced by a known power input to the sample. The results are given in Table I. Heat input to the sample produced by opening the lower mechanical switch was typically on the order of 20 to 50 ergs. The use of these two mechanical heat switches made it unnecessary to use helium exchange gas at any time during an experiment prior to make the heat capacity measurements.

Table I. Thermal resistance of the lower heat switch

T (°K)	K (erg sec^{-1} deg^{-1})	K/T^2 (erg sec^{-1} deg^{-3})
0.245	270	4500
0.570	1416	4400
1.281	8000	4900

Figure 2 shows, in schematic cross section, a diagram of the ^3He pumping line which was fabricated out of stainless steel tubing. A Welch "Duo-Seal" Type 1402-KBG 100 liter/minute mechanical vacuum pump, modified to provide a vacuum tight outlet port, was used to pump the liquid ^3He to about 0.5°K. A 300 liter/second oil diffusion pump was then used to pump the liquid ^3He to 0.24°K. In the present experiments, about 0.13 mole of ^3He was condensed into the ^3He chamber. This amount was sufficient to cool the copper block (containing about 20 moles of copper) from 1.08 to 0.24°K and to maintain the latter temperature for more than 24 hours. The heat leak into the block (at 0.24°K) from the ^4He bath (at 1.06°K) was approximately 70 erg/sec.

B. Temperature Regulation

When the block was in thermal contact with the ^4He or H_2 bath, the block temperature was regulated by regulating the bath temperature. For this purpose, two kinds of temperature regulator were used. A mechanical pressure regulator similar to the one described by Walker[1] was used to regulate the liquid H_2 bath in the temperature range 14 to 20°K, and the ^4He bath in the range 1.8 to 4.2°K. For regulating the ^4He bath at

temperatures below 1.8°K, an electronic temperature regulator similar to the one described by Sommers[2] was used. With liquid ^{4}He in the bath, the block could also be regulated at any temperature from 4.2°K to well above 20°K. This was accomplished by opening the upper heat switch and using the electronic regulator to supply sufficient power to the block to balance the heat leak from the block to the bath. For temperature below 1.2°K, temperature regulation was achieved by adjusting the rate of pumping on the liquid ^{3}He to produce a slow downward temperature drift and then using the electronic regulator to supply power sufficient to maintain a constant block temperature. Except at temperatures just above the λ point, (2.172°K), the block temperature could be held constant to within 0.01%.

C. Thermometry

Sample temperature was determined by means of a resistance thermometer placed in intimate thermal contact with the sample. The bonding agent was GE 7031 varnish. This thermometer was usually a carbon resistance thermometer consisting of a thin layer of Aquadag painted onto a Formvar insulated copper wire. However, for a few measurements a germanium resistance thermometer was used. During the course of this work, cryogenic resistance thermometers, incorporating a crystal of semiconducting germanium as the temperature sensing element, became commercially available from the Minneapolis-Honeywell Regulator Company. One of these thermometers, having a resistance of about 2000 ohms at 4.2°K, was mounted on the copper block. Over a period of several months, during which time the thermometer was cycled between 0.24°K and room temperature at least a dozen times, the reproducibility of its resistance vs temperature calibration was checked from 1.2 to 4.2°K and was found to be reproducible to within the precision

of the temperature measurements. It was then decided to use one of these germanium resistance thermometers for some of the heat-capacity measurements in the range 1.2 to 20°K since the lengthy procedure of thermometer calibration would have to be performed only once.

The DC resistance of the sample thermometer was determined with a Rubicon Double Six Dial Thermofree Potentiometer. The unbalance voltage from the potentiometer was amplified with a Keithley Model Number 149 Milli-Microvoltmeter and then displayed on a recording potentiometer. The resistance vs temperature relation for the sample thermometer was determined by calibrating it against different primary thermometers in the temperature regions discussed below.

10 to 20°K

In this temperature range, the sample thermometer was calibrated against a platinum resistance thermometer manufactured by the Leeds and Northrup Company (Serial Number 1520046) and calibrated by the National Bureau of Standards from 10 to 92°K against the NBS-1955 temperature scale. A measuring current of 5 milliamperes was employed and the resistance was determined with the same Rubicon potentiometer used with the sample thermometer. Above 14°K a temperature sensitivity of 0.03% was possible; at 10°K the sensitivity was 0.1%. During an earlier experiment, the calibration of the platinum thermometer was checked in the present apparatus by comparing the NBS calibration with the vapor pressure of 20.4°K equilibrium H_2 as given by Wooley, Scott and Brickwedde.[3] No significant difference was found.

1.25 to 4.2°K

In this temperature range, the sample thermometer was calibrated against the vapor pressure of ^4He. Vapor pressure readings were converted

to temperatures according to the 1958 ^{4}He scale of temperature.[4] For temperature measurements above the λ point (2.172°K), the vapor pressure of a small amount of ^{4}He contained in the vapor pressure bulb was used. Where the vapor pressure sensing tube passed through the main ^{4}He bath (see Fig. 1), it was surrounded by a vacuum jacket. This was done to eliminate possible error in the vapor pressure measurements due to "cold spots" on the wall of the vapor pressure sensing tube.[5] For measurements below the λ point, the vapor pressure bulb was pumped free of liquid ^{4}He (to avoid head input to the block due to superfluid film refluxing), and the vapor pressure of the main ^{4}He bath was measured. At each calibration point, the bath temperature was held constant by means of either the mechanical or the electronic regulator and, when the sample temperature had reached equilibrium, both the resistance of the thermometer and the vapor pressure were determined. Vapor pressures were measured with mercury and oil manometers, and a Wild cathetometer. A precision of 0.02 mm Hg was easily obtained. The tubes communicating from the manometers into the helium dewar were large enough that thermomolecular pressure corrections were unnecessary.

0.24 to 1.25°K

In this temperature range, the sample thermometer was calibrated against the magnetic susceptibility of a sphere of cerium magnesium nitrate ($Ce_2Mg_3(NO_3)_{12}\cdot 24H_2O$). Single crystals of cerium magnesium nitrate were grown by the slow evaporation of a saturated solution in a refrigerator at 5°C. In this way clear single crystals, approximately 0.25 inch thick and 1.5 inches in diameter, were obtained. Two of these crystals were glued together with GE 7031 adhesive varnish and machined into a hemisphere with a radius of 0.50 inch. Two such hemispheres were then glued with

GE 7031 varnish to the opposite sides of a piece of 0.005 inch thick copper foil which was soldered to the bottom of the copper sample cage. The cerium magnesium nitrate crystal was thus in good thermal contact with the copper block and, through the lower heat switch, with the sample. The cerium magnesium nitrate crystals were oriented with their hexagonal axes perpendicular to the field of the susceptibility measuring coils. Daniels and Robinson[6] have shown that the magnetic susceptibility of cerium magnesium nitrate is proportional to the inverse of the absolute temperature to temperatures well below those of interest here. In our experiments, the mutual inductance of coils surrounding the salt was measured and compared with the vapor pressure of ^{4}He in the range 1.25 to 4.2°K. A linear extrapolation of mutual inductance vs 1/T was then used to define a temperature scale below 1.2°K. The mutual inductance was determined with a 23 cps null detecting inductance bridge similar to the one described by Erickson, Roberts and Dabbs.[7] With the apparatus used in the present experiments, temperatures could be measured with a precision of 0.1% at 1°K and 0.04% at 0.3°K.

4.2 to 14°K

Also located in the copper block (but not shown in Fig. 1) are two chambers which were originally intended to be part of a constant volume gas thermometer of design similar to the one proposed by Scott, Kilgore and Gaumer.[8] It was planned to use this gas thermometer to define a temperature scale and to calibrate the "Aquadag" sample thermometer in the range 4.2 to 14°K. However, when highly stable and reproducible germanium resistance thermometers became commercially available, it was decided to construct a separate apparatus for the purpose of calibrating these thermometers from 0.25 to 20°K. One of these calibrated germanium

thermometers could then either be used as a sample thermometer or it could be mounted permanently on the copper block and used to calibrate the sample thermometer during each experiment. The calibrating apparatus is quite similar to that shown in Fig. 1 except for the omission of the lower heat switch.

Since this calibrating apparatus was not completed in time to be used in conjunction with the present experiments, a provisional temperature scale between 4.2 and 10°K was established as follows. The sample thermometer was calibrated between 1.25 and 4.2°K and between 10 and 20°K as described above. All of these calibration points were then fit by least squares to one of the polynomials

$$1/T = A+BR+CR^2+DR^3+ER^4 \qquad (1)$$

or

$$\frac{\log}{T} = A+B \log R+C \log^2 R+D \log^3 R + E \log^4 R, \qquad (2)$$

where R is the thermometer resistance and A, B, C, D and E are constants. Generally, Eq. (1) gave the best fit to the calibration data of germanium resistance thermometers, while Eq. (2) gave the best fit of the Aquadag thermometers. For each calibration point, a temperature T_c was calculated from Eqs. (1) or (2) and a plot of T_o/T_c vs T_c, where T_o is the observed calibration temperature. For both types of thermometer, the calculated temperatures differed from the observed temperatures usually by less than 0.2% and often by less than 0.05%. A smooth "difference curve" was drawn through these points and interpolated through the temperature region 4.2 to 10°K. This difference curve was a slowly varying function of T_c and its position and slope at 4.2 and 10°K were such as to define the interpolation between 4.2 and 10°K unambiguously. The "difference

curve" was then used to correct all temperatures subsequently calculated from either Eqs. (1) or (2). The validity of this interpolation procedure can only be justified by using a thermometer calibrated in this manner for measurements on a substance which has a slowly varying heat capacity of known temperature dependence in this temperature region. Such a set of measurements on a high purity sample of Cu will be discussed in Section I.

D. Procedure

The following is a brief description of a typical experiment in which heat capacities were measured from 0.25 to 20°K. The apparatus was slowly cooled from room temperature to 78°K by putting liquid nitrogen in the outer nitrogen dewar and about 500 microns of hydrogen exchange gas in the vacuum can. When the apparatus had cooled to 78°K, liquid H_2 was transferred into the inner dewar. With the hydrogen exchange gas still present, the sample thermometer was calibrated against the platinum thermometer from 14 to 20°K. For calibrating between 10 and 14°K, the hydrogen in the inner dewar was pumped to about 8°K, the hydrogen exchange gas pumped out of the vacuum can and the upper mechanical switch opened. The temperature of the block was raised above that of the bath and regulated by means of the electronic temperature regulator as discussed above. Normally 15 to 20 calibration points were taken between 10 and 20°K. When this calibration was completed, the block was recooled to about 8°K, the lower heat switch opened and heat capacity points taken up to 20°K.

The vacuum can was then pumped to a pressure of 10^{-4} to 10^{-5} mm Hg as read on an ionization gauge at the top of the pumping line, and the liquid H_2 in the inner dewar was replaced with liquid ^4He. The block and the sample were cooled to 4.2°K by means of the two heat switches. When

the sample had cooled to 4.2°K, the lower mechanical switch was opened and heat capacity points taken from 4.2 to 10°K. Both mechanical switches were then closed and the ^{4}He bath was pumped to approximately 1.06°K. The ^{3}He was then condensed into its chamber in the copper block, the upper mechanical switch opened and the block cooled by pumping on the liquid ^{3}He. At approximately 25 temperatures between 0.24 and 1.2°K, the block temperature was regulated as discussed in Section I-B and the sample thermometer calibrated against the susceptibility of the cerium magnesium nitrate crystal.

The ^{3}He was then recondensed into its chamber and the block cooled to 0.24°K. The lower mechanical switch was opened and heat capacity points taken from 0.24 to 4.2°K. As the final part of the experiment, about 20 microns of helium exchange gas were put into the vacuum can (to insure thermal equilibrium between the bath, sample and block), and both the sample thermometer and the cerium magnesium nitrate crystal were calibrated against the vapor pressure of ^{4}He between 1.25 and 4.2°K.

Heat capacities were measured in the usual way by introducing known amounts of energy into the sample while monitoring the sample temperature on a recording potentiometer. The fore and after temperature drifts of each point were extrapolated to the midpoint of the heating period to obtain the temperature increment for that point. Other procedural details not discussed here can be found in some of the recent publications from this laboratory.[9-11]

E. Accuracy of the Heat Capacity Measurements

The equipment used for resistance thermometry and to measure energy input to the sample has been thoroughly tested and the principal errors in the present measurements are expected to arise from temperature scale

errors. The temperature scales and temperature measuring techniques used between 0.24 and 4.2°K have been in use in this Laboratory for several years. Extensive heat capacity measurements on a high purity copper sample (from 0.08 to 1°K in an adiabatic demagnetization calorimeter and from 1 to 4°K in a ^{4}He calorimeter) and comparison of these measurements with those of other laboratories show that the heat capacities are accurate to better than 1%.[9,10] The heat capacity of one of the samples used in the present work ($Ti_{0.99}$ $Fe_{0.01}$) was measured from 0.25 to 1.2°K in the apparatus described here and from 0.08 to 0.8°K in the adiabatic demagnetization calorimeter mentioned above. These two sets of results agree to within the precision of the measurements (better than 2%) throughout the entire range of overlap (see Fig. 10). We therefore believe the measurements made in the ^{3}He apparatus described here to be accurate to within 1% throughout the temperature range 0.25 to 4.2°K.

Between 10 and 20°K, the accuracy of the present measurements depends on the accuracy of the NBS-1955 temperature scale, against which the platinum thermometer was calibrated. It is generally believed that this temperature scale, which is based on ^{4}He gas thermometer measurements, is accurate to within 1% over the temperature range of interest here. Between 4.2 and 10°K, the accuracy of the present measurements is limited by the accuracy with which the "difference curve" can be interpolated through this temperature region. As a check of this interpolation procedure, the heat capacity of a high purity Cu sample was measured from 1.2 to 20°K in the present apparatus, using a carbon resistance sample thermometer calibrated as described in Section I-C. The data varied smoothly with temperature and could be represented to within 1%, in the temperature range 1.2 to 10°K, by the equation

$$C = \gamma T + \alpha T^3, \qquad (3)$$

with $\gamma = 0.684$ mJ mole^{-1} deg^{-2} and $\alpha = 0.0496$ mJ mole^{-1} deg^{-4}. For comparison, the constants γ and α obtained from other recent heat capacity measurements on Cu are summarized in Table II. From 10 to 20°K, the data increasingly deviated from Eq. (3) as the T^5 and T^7 terms in the lattice heat capacity became larger. The absence of any pronounced "anomalies" in the measured heat capacity between 4.2 and 10°K justifies the use of this interpolation to establish a temperature scale in this region.

Table II. Summary of recent heat capacity measurements on copper at liquid helium temperatures.

	γ (mJ mole^{-1}deg^{-2})	α (mJ mole^{-1}deg^{-4})
This work	0.684	0.0496
Phillips[a]	0.695	0.0480
Corak et al.[b]	0.688	0.0478
Rayne[c]	0.686	0.0473
Griffel et al.[d]	0.691	0.0486
Ramanathan and Srinivasan[e]	0.720	0.0523
Manchester[f]	0.696	0.0478
du Chatenier & de Nobel[g]	0.721	0.0500
Kneip[h]	0.698	0.0482
Hake[i]	0.700	0.0469

a N. E. Phillips, Phys. Rev., 134, A385 (1964).

b W. S. Corak, M. P. Garfunkel, C. B. Satterthwaite and A. Wexler, Phys. Rev., 98, 1699 (1955).

c J. A. Rayne, Australian J. Phys., 9, 189 (1956).

d M. Griffel, R. W. Vest and J. F. Smith, J. Chem. Phys., 27, 1267 (1957).

e K. G. Ramanathan and J. M. Srinivasan, J. Sci. Ind. Res. (India), 16B, 277 (1957).

f F. D. Manchester, Can. J. Phys., 37, 989 (1959).

g F. J. du Chatenier and J. de Nobel, Physica, 28, 181 (1962).

h G. Kneip (private communication).

i R. R. Hake, Phys. Rev., 123, 1986 (1961).

II. THE HEAT CAPACITY OF RUTHENIUM

For Hg,[12,13] Sn,[14,15] Tl,[16] Pb,[17] In,[18] Zn[19] and Cd,[20] the superconducting transition temperature T_c is related to the isotopic mass M by the relation

$$T_c \propto M^{-\alpha}, \qquad (4)$$

with $\alpha \approx 0.5$. These experimental results confirmed Frohlich's[21] suggestion that superconductivity is the result of an electron-phonon interaction, and suggested the basis for the present BCS theory of superconductivity. Recently it was discovered that the parameter $\alpha \approx 0$ for Ru[22,23] and is between 0 and 0.5 for Os[19,24] and Mo.[25] These findings have led to speculation that mechanisms other than the electron-phonon interaction may be responsible for superconductivity in the transition metals and to a reexamination of the assumptions and approximations used in the original BCS theory.[26-28] It was therefore of considerable interest to compare the parameters characteristic of the superconducting state of Ru with those of other superconductors.

We have measured the heat capacity of Ru from 0.27 to 1.0°K. The sample was a 4.9325-g (0.048802 mole) arc-melted pellet obtained from Dr. T. H. Geballe of Bell Telephone Laboratories. Spectrochemical analysis showed the sample to contain between 10 and 50 ppm of Fe, Mn and Pd and less than 10 ppm of Al, Cu, Mg and Ni. Most of the experimental points are shown in Fig. 3 as a plot of C vs T. The normal-state heat capacity (measured in a magnetic field of 225 Oe) is proportional to T, indicating that the lattice heat capacity is negligible in this temperature range. The slope of the straight line that best fits the normal state points gives the value 2.98 mJ $mole^{-1}$ deg^{-2} for γ, the

coefficient of T in the normal-state electronic heat capacity. Figure 4 shows some additional points taken with small temperature increments for the purpose of determining the width and temperature of the superconducting transition. The transition is complete within an interval of 0.006°K and is centered at 0.471°K.

The BCS expression for the superconducting-state electronic heat capacity C_{es} can be approximated by

$$\frac{C_{es}}{\gamma T_c} = a \exp(-bT_c/T), \qquad (5)$$

where the parameters a and b are slowly varying functions of T/T_c and can be taken as constants within a restricted temperature interval. Figure 5 shows a semi-logarithmic plot of the experimental $C_{es}/\gamma T_c$ vs T_c/T. The present measurements do not extend far enough into the range of T_c/T, where a and b are usually evaluated to determine the values of these parameters uniquely. The straight line shown in Fig. 5 fits the lowest temperature superconducting-state points and has a slope that makes the entropies of the normal and superconducting states equal at T_c as required by the third law of thermodynamics. In the present case such a procedure determines a and b quite precisely because more than 70% of the superconducting-state entropy at 0.27°K is in the temperature region just below 0.27°K, thus making the calculated superconducting-state entropy at T_c very sensitive to the slope of the extrapolation.

Smoothed experimental values of C_{es}, extrapolated to T = 0°K using Eq. (5) with a = 8.12 and b = 1.40, were used to calculate the free energy difference between the normal and superconducting-states $\Delta F(T)$, and the critical field $H_c(T)$, according to the thermodynamic relation

$$\Delta F(T) = \frac{V_m H_c^2(T)}{8\pi} = \int_{T_c}^{T} dT \int_{0}^{T} \left(\frac{\gamma T - C_{es}}{T}\right) dT, \qquad (6)$$

where V_m is the molar volume. At T=0°K, the free energy difference is $\Delta F_o = 0.153$ mJ mole^{-1}. Since low-temperature thermal expansion data for ruthenium are not available, the room-temperature molar volume $V_m = 8.15$[29] cm^3 mole^{-1} was used to calculate the value 68.5 Oe for H_o, the critical field at T=0°K. The error in H_o resulting from this approximation should be less than 1%. The deviation of the critical field from parabolic temperature dependence is shown in Fig. 6 as a plot of $D(t) = h-(1-t^2)$ vs t^2, where $h = H_c/H_o$ and $t = T/T_c$. The maximum deviation $D_m = -0.043$ occurs at $t = 0.7$.

Table III summarizes the comparison of our data with other related measurements on ruthenium. The error limits quoted for the present results are estimates intended to include systematic errors in temperature measurement and also possible errors arising from scatter in the experimental points. The five values listed for T_c are in reasonable agreement considering the difficulties encountered in producing pure, strain-free samples and in measuring temperatures below 0.5°K. The value of H_o reported here depends on the extrapolation of C_{es} to T=0°K, but the requirement that the extrapolation be consistent with the third law of thermodynamics makes significant error unlikely. The magnetic determinations of H_o all make use of an assumed parabolic temperature dependence for H_c which can introduce appreciable error into the value for H_o. In addition, the effects of strains, impurities and non-cylindrical sample shape may considerably broaden the superconducting to normal-state transition in a magnetic field and introduce some ambiguity into the magnetic determination of H_c.

Table III. Summary of Low Temperature Calorimetric and Magnetic Measurements on Ruthenium

	C, H_c [a]	H_o (Oe)	T_c (°K)	γ (mJ mole^{-1} deg^{-2})	$C_{es}(T_c)-\gamma T_c$ (mJ mole^{-1} deg^{-1})	sample purity (%)
This Work	C	68.5	0.471 ±0.002	2.98 ± 0.04	1.9	99.99
N.M. Wolcott[b]	C			3.35		99.98
J.A. Carruthers[c] and A. Connolly	H_c	66	0.49	2.43		not stated
T.H. Geballe[d] et.al.	H_c		0.493			99.99
D.K. Finnemore[e] & D.E. Mapother	H_c	62	0.477		2.2	same samples as Ref. d
J.K. Hulm and B. B. Goodman[f]	H_c	46	0.47	1.2		99.99

Table III (continued)

[a] C denotes calorimetric measurements; H_c denotes critical field measurements.

[b] N. M. Wolcott, Conference de physique des basses temperatures, Paris, 1955 (Centre de National de la Recherche Scientifique and UNESCO, Paris, 1956) p. 286.

[c] J. A. Carruthers and A. Connolly, Proceedings of the Fifth International Conference on Low Temperature Physics and Chemistry, Madison, Wisconsin, August 30, 1957, J. R. Dillinger (ed),(Univ. of Wisconsin Press, Madison, 1958), p. 276.

[d] See Ref. 22.

[e] See Ref. 23.

[f] J. K. Hulm and B. B. Goodman, Phys. Rev., 106, 659 (1957).

The samples used by Finnemore and Mapother apparently showed more nearly ideal magnetic transitions than those used in the other H_c measurements, but their accuracy was still somewhat limited by the near-spherical shape of their samples. This limitation and the fact that their measurements extend only to the temperature of the maximum deviation of the critical field from a parabola could account for the discrepancy between their H_o and that reported here. There is, however, a significant discrepancy in the values of $C_{es}(T_c) - \gamma T_c$. The very low values of H_c observed by Hulm and Goodman suggest that the flux penetration into their samples was incomplete at their reported values for H_c.

The discrepancies between the γ value reported here and those derived from critical field measurements are not surprising since the accuracy of the latter values depends on an accurate knowledge of the shape of the critical field curve near T=0°K. None of the critical field measurements listed in Table III extended to low enough temperatures to precisely define the shape of the critical field curve in that temperature region.

For the purpose of comparing Ru with other superconductors, values for several parameters characteristic of the superconducting-state are summarized in Table IV, which includes most recent calorimetric and critical field measurements. These data are judged to be the most reliable presently available on the basis of close agreement between independent determinations and/or the use of well established experimental techniques. The entries in this table are arranged according to ascending values for T_c/θ_o, since correlations between T_c/θ_o and deviations from BCS behavior have been pointed out. Goodman has drawn attention to a correlation between the parameter $\eta = V_m H_o^2/8\pi\gamma T_c^2$ and T_c/θ_o, and the positive D(t) curves for mercury and lead have frequently been associated

with their large T_c/θ_o values. Examination of Table IV shows no anomalous behavior of Ru relative to the other superconductors and, in particular, relative to the non-transition metal superconductors that show a normal isotope effect.

Figure 7 is a plot of $V_m H_o^2/8\pi\gamma T_c^2$ and $2\epsilon(o)/kT_c = (2\pi V_m/3\gamma)^{1/2}(H_o/T_c)$ vs T_c/θ_o of the type given by Goodman, but including only data from Table IV. Goodman's original plot contained much apparently unreliable data (as indicated by the very large error bars shown for most of the points) and suggested a linear correlation between $2\epsilon(o)/kT_c$ and $\ell n\ T_c/\theta_o$. The nature of the correlation indicated by Fig. 7 is quite different: for $T_c/\theta_o < 0.02$, $2\epsilon(o)/kT_c$ is approximately independent of T_c/θ_o and only slightly less than the BCS value in the weak-coupling limit, i.e. $3.52\ kT_c$; only for $T_c/\theta_o > 0.02$ do the points rise appreciably above the weak-coupling value. This changes considerably the probable significance of the correlation. Since deviations from the BCS law of corresponding states are important only for large T_c/θ_o, they are probably a result of the mathematical approximations in the theory rather than an indication of a more fundamental approximation.

Plots of $C_{es}(T_c)/\gamma T_c$ and D_m, the maximum value of D(t), are not given here, but they show a correlation with T_c/θ_o very similar to that shown by $2\epsilon(o)/kT_c$. These parameters are all related to the deviation of H_c from parabolic temperature dependence. From Eq. (6) it follows that

$$\Delta C = C_n - C_s = -\frac{V_m T}{8\pi}\frac{d^2 H_o^2}{dT^2}, \qquad (7)$$

and the substitutions $H_c = H_o(1-t^2) + D(t)$, $t^2 = y$, $D' = dD/dy$,

Table IV Summary of parameters characteristic of the superconducting state for several superconductors

	C,H_c [a]	$T_c/\theta_o X10^2$	a	b	D_m [b]	$\frac{\gamma T_c^2}{V_m H_o^2}$	$\frac{C_{es}}{\gamma T_c}$	Ref.
Ru	C	0.078	8.12	1.40	-0.043	0.172	2.35	c
Cd	C	0.248	6.2	1.26	-0.046	0.177	2.32	d
Al	C	0.272	7.1	1.34	-0.040	0.173	2.43	e
Zn	C	0.276	6.4	1.27	-0.043	0.177	2.30	f
	C		5.8	1.22	-0.050	0.183		g
Ga	C	0.332	7.46	1.39	-0.035	0.169	2.44	d
	C	0.343	7.0	1.35	-0.036	0.170	2.41	f
V	C	1.49	9.17	1.50	-0.031	0.164		h
Sn	C	1.85	7.63	1.41	-0.026	0.164	2.68	i
	C	1.91	9.17	1.50	-0.024	0.161		j
	H_c				-0.026	0.161		k
In	C	3.07	8.25	1.34	-0.021	0.158		l
	H_c				-0.020	0.156		k
Nb	C	3.35	8.21	1.52		0.154	2.87	m
Hg^{α}	C	5.71						n
	H_c				+0.017			k
	H_c				+0.014	0.138		o
Hg^{β}	H_c							
Pb	H_c	6.87			+0.023	0.139	3.63	p,q

Table IV (continued)

[a] C denotes calorimetric measurements; H_c denotes critical field measurements.

[b] D_m is the maximum deviation of the critical field curve from a parabola.

[c] This work. Value for θ used to compute T_c/θ came from N. M. Wolcott (see Ref. b of Table III); for value of V_m at 20°C, see Ref. 29.

[d] N. E. Phillips, Phys. Rev., 134, A385 (1964).

[e] N. E. Phillips, Phys. Rev., 114, 676 (1959).

[f] G. Seidel and P. H. Keesom, Phys. Rev., 112, 1083 (1958).

[g] N. E. Phillips, Phys. Rev. Letters, 1, 363 (1958).

[h] W. S. Corak, B. B. Goodman, C. B. Satterthwaite and A. Wexler, Phys. Rev., 102, 656 (1956).

[i] C. A. Bryant and P. H. Keesom, Phys. Rev., 123, 491 (1961).

[j] W. S. Corak and C. B. Satterthwaite, Phys. Rev., 102, 662 (1956).

[k] D. K. Finnemore and D. E. Mapother, Report No. 2, OOR Project No. 2771-P.

[l] H. R. O'Neal and N. E. Phillips (to be published).

[m] H. A. Leupold and H. A. Boorse, Phys. Rev., 134, A1322 (1964).

[n] M. H. Lambert and N. E. Phillips (to be published).

[o] J. E. Schirber and C. A. Swenson, Phys. Rev., 123, 1115 (1961).

[p] D. L. Decker, D. E. Mapother and R. W. Shaw, Phys. Rev., 112, 1888 (1958).

[q] θ_o = 105°K for Pb, W. R. Gardner and N. E. Phillips (to be published).

$D'' = d^2D/dy^2$, and

$V_m H_o^2/2\Pi T_c^2 = \gamma_p$ (γ_p is the value of γ corresponding to a parabolic critical field curve) give

$$\Delta C = - \gamma_p T \left[(D+1)(D'-1) + t^2 \{2D''(D+1)+2D'^2-5D'-1\}-2t^4 D''\right] \quad (8)$$

From the assumption that C_{es} goes to zero more rapidly than T as T goes to zero it follows that

$$\gamma = \lim_{t \to 0} \frac{\Delta C}{T} = \gamma_p \{1-D'(0)\}, \quad (9)$$

and

$$\eta = \frac{1}{4} \frac{\gamma_p}{\gamma} = \frac{1}{4} \{1-D'(0)\}^{-1} , \quad (10)$$

or

$$\eta \approx \tfrac{1}{4}(1+D'(0)). \quad (11)$$

At t = 1, Eqs. (8) and (9) give

$$\frac{C_{es}(T_c)}{\gamma T_c} = \frac{\gamma T_c - \Delta C(T_c)}{\gamma T_c}$$

$$= 1 + 2 \frac{\{1-D'(1)\}^2}{1-D'(0)} \quad (12)$$

$$\approx 3 - 4D'(1) + 2D'(0). \quad (13)$$

The similarity of the correlations of η, D_m and $C_{es}(T_c)/\gamma T_c$ with T_c/θ_o is an indication that the D(t) curves for different superconductors have roughly the same shape (but different amplitudes, D_m) and that the main features of the critical field curves conform to a law of corresponding states if a parameter, say $2\epsilon(0)/kT_c$, that depends on T_c/θ_o is included.

Apart from the absence of an isotope effect, the superconducting transition in Ru appears to be no different from those of the non-transition

metals, including those that show a normal isotope effect. The parameters characterizing the critical field curve (and therefore the thermodynamics of the transition) of different superconductors vary in a regular manner with T_c/θ_o and Ru fits into this correlation quite accurately.

III. THE HEAT CAPACITY OF Ti-Fe ALLOYS

In 1958 Matthias et.al.[31] demonstrated that small amounts of the magnetic lanthanide elements dissolved in lanthanum depressed the superconducting transition temperature of that element by an amount that was correlated with the net 4f electron spin of the solute atom. Thus Gd with a spin of 7/2 depressed the transition temperature ten times as much as did Tm with a spin of one, even though both elements have the same magnetic moment. In 1959 Matthias et.al.[32] found that the transition temperature of Ti could be increased by an order of magnitude by the addition of small (viz. 1-5 at %) amounts of the magnetic transition metals Mn, Cr, Co and Fe. On the basis of these findings Matthias et.al.[32] and Geballe[33] have suggested that, since magnetic impurities raise the transition temperature of Ti but lower the transition temperature of La, a difference might exist between the mechanisms responsible for superconductivity in the rare earths and in the transition metals. They suggested that an interaction between the 3d and conduction electrons might supplement or even replace the usual BCS electron-phonon interactions as the cause of superconductivity in the transition metals.

In view of the differing behavior exhibited by La and Ti when alloyed with magnetic elements, and in view of the potential importance of the suggestions made by Matthias and Geballe to the theoretical treatment of superconductivity, it was of considerable interest to do further experimental work on some of the systems discussed above. Several samples of the Fe-Ti alloy system, similar to the ones used by Matthias et.al.[32] on their earlier investigations, were supplied by Dr. T. H. Geballe of the Bell Telephone Laboratories. Heat capacity measurements were made on them to determine if the high transition temperatures observed by Matthias et.al.

are bulk properties of the samples. The magnetic measurements, used by Matthias et.al. to detect superconductivity, showed the superconducting transition to be accompanied by an apparently complete diamagnetic transition, and they therefore assumed the superconductivity to be a true bulk effect. However, it is entirely possible that a suitable arrangement of interconnected superconducting filaments can produce complete diamagnetic shielding even though only a relatively small fraction of the sample volume is superconducting. Heat capacity measurements can, in principle, differentiate between a complete and partial volume superconducting transition.

Heat capacity measurements were carried out on samples of the alloy system Fe_xTi_{1-x} with x = 0, 0.0005, 0.0025 and 0.01. (Hereafter sample composition will be denoted as x% Fe-Ti.) The measurements on the 0.05% and 0.25% Fe-Ti alloy samples covered the temperature range 0.25 to 4.2°K; and on the 1.0% Fe-Ti sample, the range 0.25 to 20°K. These measurements were carried out in the ^{3}He cryostat described in Part I. The measurements on "pure" Ti (0.2 to 1.2°K) and an additional set of measurements on the 1.0% Fe-Ti alloy (0.08 to 0.8°K) were made in an adiabatic demagnetization calorimeter.[10]

The heat capacity of Ti is presented in Fig. 8 as a plot of C vs T, and the results are compared with other recent work in Table V. The present measurements on pure Ti were made primarily to provide a value for γ for comparison with the γ values of the Fe-Ti alloys. The normal-state heat capacity (measured in a magnetic field of 275 Oe is proportional to T, indicating that the lattice-heat capacity is negligible at these temperatures. The slope of the best straight line fit to the normal-state points gives a value for γ of 3.41 ± 0.03 mJ mole^{-1} deg^{-2}. The calorimetrically determined values for γ, except that found by Wolcott, are in reasonable agreement

Table V Summary of Low Temperature Calorimetric and Magnetic Measurements on Titanium

	C, H_c[a]	Θ_o	γ	T_c	H	Sample Purity
	(°K)	(°K)	(mJ $mole^{-1}deg^{-2}$)	(°K)	(Oe)	(%)
This work			3.41 ± 0.03	0.33		>99.99
						≈ 9 ppm Fe
						≈4 ppm Mn
R. L. Falge[b]	H_c		3.2	0.42	56	< 5 ppm Mn
						< 2 ppm Fe
I. Estermann et. al.[c]	C	280	3.34			> 99
M. C. Steel and R. A. Hein[d]	H_c			0.37	86	99.98
T. S. Smith and J. G. Daunt[e]	H_c			0.558		99.95
T. S. Smith[f] et. al.	H_c			0.387	20	99.99
G. D. Kneip[g] et.al.	C	430	3.35			99.86
N. M. Wolcott[h]	C	430	3.56			99.98
R.R. Hake[i] and J. A. Cape	C	429	3.30			99.92

Table V (continued)

[a] C denotes calorimetric measurements; H_c denotes critical-field measurements.

[b] R. L. Falge Jr. Phys. Rev. Letters, 11, 248 (1963).

[c] I. Estermann, S. A. Friedberg and J. E. Goldman, Phys. Reb., 87, 582 (1952)

[d] M. C. Steele and R. A. Hein, Phys. Rev., 92, 243 (1953).

[e] T. S. Smith and J. C. Daunt, Phys. Rev., 88, 1172 (1952).

[f] T. S. Smith and W. B. Gager and J. G. Daunt, Phys. Rev., 89, 654 (1953).

[g] G. D. Kneip, Jr., J. O. Betterton, Jr., and J. O. Scarbrough, Phys. Rev., 130, 1687 (1963).

[h] See Ref. b of Table III.

[i] R. R. Hake and J. A. Cape (preprint of work to be published).

with the value reported here. The magnetically determined values for γ are subject to the same errors discussed in connection with Ru (see Section II). The superconducting-state heat capacity was measured in a magnetic field of less than 0.1 Oe. The transition was 0.060°K wide and was centered at 0.33°K. The discontinuity in the heat capacity at 0.33°K was 1.2 mJ $mole^{-1}$ deg^{-1}. The width of the transition made it impractical to derive other superconducting state parameters from the present data. The values for T_c listed in Table V show a fairly large scatter. This is not surprising considering the difficulty of preparing pure, strain free samples. It has been shown[34] that traces of Mn lower the transition temperature of Ti, while larger amounts raise the transition temperature. The large scatter in the reported values for T_c can perhaps be attributed to the differing purities of the samples used. We are inclined to view Falge's value for T_c of 0.42°K as the most reliable since his sample appeared to be exceptionally pure and strain free.

Before meaningful conclusions can be drawn from the present results on the Fe-Ti alloy system and related work on Fe-, Mn-, Cr- and Co-Ti alloys, a brief summary of the metallurgy of these systems must be given. Since these four alloys are quite similar the discussion will be limited to the Fe-Ti system.[35] A phase diagram of the Ti-rich portion of the Fe-Ti alloy system is presented in Fig. 9. It must be emphasized that, since the phase boundaries are not accurately known, only semi-quantitative conclusions can be drawn from Fig. 9. At room temperature, pure Ti has a hexagonal close packed (hcp) lattice structure (the α phase) which transforms to a body centered cubic (bcc) structure (the β phase) at 882°C. By adding small amounts of Fe, one, two or three phases can be produced depending on the Fe concentration and the heat treatment given the sample.

The phase diagram indicates that the 0.05% Fe-Ti sample used in the present measurements, which was annealed at 700°C for 14 days, contains pure α (hcp) phase. However, since the solubility limit of Fe in α-Ti at 700°C is not accurately known, the presence of small amounts of the iron-rich β (bcc) phase cannot be ruled out. Shortly after the present heat capacity measurements were completed, the 0.05% Fe-Ti sample was examined by standard optical metallographic and X-ray fluorescence microprobe techniques. Examination showed this sample to contain small amounts (<0.1%) of iron rich phase (> 15% Fe) present as inclusions, with diameters of $\approx$ 1-2 microns, in the bulk α phase. At present these inclusions have not been further characterized.[36]

The 0.25% Fe-Ti sample, which was quenched from the melt to room temperature, is expected to consist of pure martensitic hcp (α') phase, formed from the parent β phase as the sample is cooled below the M_s temperature. The α' phase is highly strained, supersaturated and metastable, with lattice constants similar to those of pure α-Ti. Metallographic examination confirmed that the sample consisted of pure α' phase.[36]

On the basis of Fig. 9, the 1% Fe-Ti sample, which was annealed at 700°C for 6 days, is expected to be a mixture of the α and of the iron-rich β phases in the approximate ratio of 9:1. However, metallographic examination showed the sample to be more than 99.9% pure α' phase. This discrepancy can be attributed[36] to the fact that the sample was quenched to room temperature from the melt and then annealed at 700°C without subjecting it to cold-work, thus stabilizing the α' phase.

The heat capacities of the 0.05%, 0.25% and 1.0% Fe-Ti samples are presented in Figs. 10, 11, 12 and 13 as plots of C/T vs T^2. The relevant physical and chemical characteristics of these samples, together with the

results of the present measurements and the magnetic measurements made at Bell Telephone Laboratories, are summarized in Table VI.

The slopes of the C/T vs T^2 plots should not be taken as an accurate measure of the lattice heat capacities of these alloys. Because of the small size ($\approx$ 0.05 mole) and high Debye temperature ($\approx$400°K) of these samples, the T^3 term in the heat capacity of the addenda (which consisted mainly of a copper sample holder and the GE 7031 varnish used to provide thermal contact between the sample and the holder) amounted to approximately 75% of the total T^3 heat capacity. Since the value of the T^3 term in the heat capacity of the varnish is known only approximately, considerable error is introduced into the T^3 term in the heat capacity of the sample.

Each sample shows a small T^{-2} term in its heat capacity at very low temperatures. This term is unaffected by a magnetic field of 300 Oe and we assume that it is a hyperfine contribution. However, its origin is not clear. The known transition metal impurity with a large nuclear moment (Mn) is present in too small an amount to account for it. If the Fe had a local moment, it could produce a hyperfine field on neighboring Ti nuclei, but the size of the T^{-2} term is uncorrelated with Fe content. A nuclear electric quadrupole contribution would be expected to be the same in all samples except for the possible effects of strain or differences in lattice parameters between the α and α' phases.

The γ values for the Fe-Ti alloys are listed in Table VI. The error limits quoted are intended to indicate errors due to the scatter in the experimental points, any errors due to temperature scale being small by comparison. The 0.05% Fe-Ti sample has a γ value (within experimental error) equal to that of pure Ti. The increase in the γ value for 0.25% Fe-Ti over that for pure Ti lies just outside the range of experimental error. These results indicate that Fe, in concentrations of up to at least 0.25%,

TABLE VI. Properties of the Fe-Ti Alloy samples used in the present experiments

Sample	Impurities[a]	Heat Treatment[a]	Phase Composition[a]	γ ($mJ\ mole^{-1}\ deg^{-2}$)	$T_c(C)$ (°K)	$T_c(M)$[a] (°K)	% Transition	$C_{es}(T_c)-\gamma T_c$ ($mJ\ mole^{-1}\ deg^{-1}$)
Ti (Bell Labs #5246	9.2 ppm Fe 4.0 ppm Mn	arc melted	α	3.41±0.03	0.33			
$Ti_{0.9995}Fe_{0.0005}$	1.2 ppm Mn	cold worked and annealed 14 days at 700°C	≈99%α	3.36±0.05	≈3	≈3	≈5	<0.5
$Ti_{0.9975}Fe_{0.0025}$	≈4 ppm Mn	quenched	α'		none	2.0 to 2.6	100	0
$Ti_{0.99}Fe_{0.01}$ (Bell Labs #4442)	~4 ppm Mn	Annealed 6 days at 700°C without cold-work	>99.9%α'	3.25±0.03 (<1°K) 3.85±0.10 (>4°K)	3	≈2.6	100	≈1.7

[a] T. H. Geballe (Private Communication).

$T_c(C)$ denotes superconducting transition temperature determined calorimetrically.

$T_c(M)$ denotes superconducting transition temperature determined magnetically.

% Transition denotes the apparent percentage of the sample volumen participating in the superconducting transition as judged by magnetic measurements.

has little effect on the density of states in hcp Ti. The heat capacity of the 1.0% Fe-Ti sample showed two linear regions when plotted as C/T vs T^2. A value for γ of 3.25 mJ mole $^{-1}$ deg $^{-2}$ was derived from the low temperature region and a value 3.85 ± 0.10 mJ mole $^{-1}$ deg $^{-2}$ was derived from the high-temperature region. The relatively large error associated with the latter value is due to the fact that the C/T vs T^2 plot is only approximately linear at these temperatures (due to the T^5 term in the heat capacity of the GE 7031 varnish), making an accurate straight line extrapolation to $T^2 = 0$ difficult.

Table VI and Figs. 10-13 clearly indicate that there are no heat capacity anomalies (in the temperature range of the present measurements) that can be associated with bulk superconducting transitions of the usual kind. Assuming the BCS relation $\frac{C_{es}(T_c)}{\gamma T} = 2.43$ to be applicable to these systems and assuming a value for γ of 3.4 mJ mole^{-1} deg $^{-2}$, one would expect a discontinuity in the heat capacity of about 12 mJ mole^{-1}deg^{-1} at 2.5°K (the approximate superconducting transition temperature given by magnetic measurements[32]) for both the 1% and 0.25% Fe-Ti alloys. The observed values are ≈ 1.7 mJ mole $^{-1}$deg^{-1}and ≈ 0 for the 1% and 0.25% Fe-Ti samples, respectively. Even allowing for the probable broadening of the transition in an alloy, it is clear that no anomalies approaching the expected size occur.

We attribute the small anomaly observed in the heat capacity of the 0.05% Fe-Ti sample at $T^2 \approx 9(°K)^2$ (see Fig. 10) to a superconducting transition occurringin some minor phase present in the sample (possibly the iron rich inclusions detected by the X-ray microprobe). The scatter of the experimental points in this region is due to the occurrence of hysteresis as the sample was cycled through this temperature region. The reason for

this hysteresis is not known. Magnetic measurements also detected a small superconducting transition (≈ 5% of the sample volume) at these temperatures.[36]

The heat capacities of both the 0.05% Fe- and 0.25% Fe-Ti alloys contain a linear term with a coefficient quite close to that for pure, normal-state Ti, indicating that the bulk hcp phase of both alloys remains in the normal-state down to the lowest temperature reached in the present measurements (0.25°K).

For the 1% Fe-Ti alloy a distinct anomaly in the heat capacity occurs near 3°K, the temperature at which magnetic measurements show a bulk superconducting transition. On the other hand, the apparent γ value on the low temperature side of the anomaly is 85% of that on the high temperature side. A magnetic field of 1500 Oe had no effect on the heat capacity anomaly.[40] Abrikosov and Gorkov[41] have predicted that magnetic impurities might produce "gapless superconductivity" with a linear term in the superconducting-state electronic heat capacity, but the situation they considered is clearly different from that existing in the present case. The theory applies to free magnetic spins, and, while there is some evidence from electron transport properties for localized moments on Fe dissolved in Ti,[39] any such moments would have to be strongly antiferromagnetically coupled to explain the observed magnetic susceptibility.[37]

The more obvious interpretation of the heat capacity of the 1% Fe-Ti sample is that the observed superconductivity is not a property of the hcp phase, but is due to a small amount of a second phase. This point of view is strongly supported by the constancy of the superconducting transition temperature for the 0.05%, 0.25% and 1% Fe-Ti samples, as observed either calorimetrically or magnetically. It is also suggested by analogy with

The Mn-Ti system for which the addition of small amounts of Mn depresses subscript in the α phase and the superconductivity reported for Mn concentrations of the order of 1% or more is due to inclusions of the β phase.[37-39] However, the analogy is not exact because magnetic susceptibility measurements suggest the existence of localized magnetic moments as the explanation of the depression of T_c in the Mn-Ti system, but show no local moments in the Fe-Ti system.[37] Furthermore, no β phase can be detected in the 1% Fe-Ti sample: metallographic examination puts an upper limit of 0.1% to the amount of β phase present and no iron-rich phase is detected by the X-ray fluorescence electron microprobe.[36] Since only a very small amount of a second phase can be present, its γ value would have to be very high to account for 15% of the linear term in the heat capacity at temperatures above the anomaly.

Recent heat capacity experiments by Heiniger and Muller[42] on 1% and 1.5% Fe-Ti give results similar to those reported here except that their measurements do not extend to low enough temperatures to observe the linear term in the region below the anomaly and they estimate a 30% transition from the size of the peak in the heat capacity.

In conclusion, it appears that dissolving small amounts of the magnetic lanthanide elements in La and small amounts of Mn in hcp Ti produces a similar effect on the superconducting transition temperature. The depression of the transition temperature in La was traced to an interaction between the 4f electron spins and the conduction electrons, and the depression of the transition temperature of hcp Ti-Mn has been attributed to the localized moments of the unpaired 3d electrons of Mn. The present experiments can best be interpreted as demonstrating the similarity in the behavior of the dilute Mn-Ti and Fe-Ti alloys. Furthermore, there is a

reasonable correlation between the occurence of superconductivity above 1°K and β phase inclusions in the Mn-Ti system but not in the Fe-Ti system.

Much work remains to be done on these Ti alloy systems. In particular, metallurgical techniques must be improved to provide for accurate and reproducible sample preparation and characterization. The Co-, Cr- and Ni-Ti alloy systems must be further investigated before reliable generalizations can be made concerning the effects of magnetic impurities on superconductivity in Ti. Also, the reason for the increase in the transition temperature of the β(bcc) phase of the Mn-Ti alloys remains unclear.

IV. THE HEAT CAPACITY OF YOs_2-$GdOs_2$ SOLID SOLUTIONS

Since externally applied magnetic fields of a few hundred Oe are often sufficient to destroy superconductivity, it was generally thought that ferromagnetic materials, in which very large internal magnetic fields are present, would not exhibit superconductivity. However, Matthias, Suhl and Corenzwit,[43] while investigating superconductivity in lanthanum - rare earth solid solutions, noticed that electronic configurations favorable to the occurrence of superconductivity were also favorable to the occurrence of ferromagnetism. For example, dilute solutions of Gd in the superconductors La and Th showed ferromagnetic behavior at low temperatures, whereas solutions of Gd in Y, a nonsuperconductor, showed no ferromagnetism. In pursuing these investigations, Matthias and co-workers found several systems in which superconductivity and ferromagnetism apparently occurred simultaneously. These systems included Gd_xLa_{1-x},[43,44] $Ce_{1-x}Pr_xRu_2$ and $Ce_{1-x}Gd_xRu_2$,[45,46] $Th_{1-x}Gd_xRu_2$,[47] and $Y_{1-x}Gd_xOs_2$.[48]

In the above work, ferromagnetic Curie points and superconducting transition temperatures were determined by magnetic susceptibility measurements. However, by this method the fractions of the sample volume participating in the ferromagnetic and superconducting transitions could not be determined. Determination of these volume fractions is of particular interest since it can be argued that the superconductivity and ferromagnetism do not coexist within the same volume element of the sample; but rather that the sample consists of many domains, some of which are superconducting and others ferromagnetic. In some circumstances a decision between these two possibilities can be made on the basis of heat capacity measurements. Preliminary measurements between 1.2 and

4.2°K by Phillips and Matthias[49] on two samples of the composition $Y_{0.96}Gd_{0.04}Os_2$ and $Y_{0.925}Gd_{0.075}Os_2$ showed that the entropy between 1.2 and 4.2°K was about 50% of the value xRln8 expected for complete alignment of the Gd spins, and that the heat capacity anomalies attributed to the superconducting transitions were roughly of the size expected on the basis of BCS theory. These results were interpreted as being consistent with the simultaneous existence of ferromagnetism and superconductivity throughout the entire sample volume.

Since a considerable portion of the entropy associated with the alignment of the Gd spins occurs outside the temperature range 1.2 to 4.2°K, it was of interest to extend the measurements to below 1.2°K and to above 4.2°K to determine this entropy more accurately. Furthermore, it was hoped to obtain a value for γ from the normal state measurements at low temperatures. The results of these experiments are shown in Figs. 14, 15 and 16. The measurements below 1.2°K were made with an Aquadag sample thermometer and above 1.2°K with a germanium resistance thermometer (MHSP 4401-648). The present results between 1.2 and 4.2°K are practically identical with those obtained by Phillips and Matthias,[49] to which the reader is referred for additional discussion.

The total entropy associated with each of the heat capacity curves shown in Figs. 14 and 15 was obtained by plotting C/T vs T, extrapolating to 0°K and performing a graphical integration. To separate the magnetic contribution, the entropy associated with the lattice vibrations and conduction electrons must be subtracted from the total entropy. Although the low-temperature heat capacity of both samples decreases precipitously, indicating rapid completion of the Gd spin alignment, the magnetic contribution to the heat capacity is still so large that a direct determination

of the normal-state electronic heat capacity is impossible. The lattice contribution to the specific heat had to be determined in the temperature range above the magnetic anomaly. To separate the lattice heat capacity, it was assumed that the magnetic heat capacity was proportional to T^{-2} in the region above the anomaly, that the lattice heat capacity was proportional to T^3 and that the normal-state electronic heat capacity was negligible. When plotted as CT^2 vs T^5, the data in the region above the anomalies gave approximately straight lines. The slopes of these lines yielded the values 200°K and 183°K for the Debye temperatures for the 7.5% Gd and 4% Gd samples, respectively.

The magnetic entropies calculated from 0 to 18°K, using the above values for the Debye temperature and assuming values for γ of 0 and 5 mJ $mole^{-1}$ deg^{-2}, are given in Table VII, along with the values of $xR\ln 8$, the entropy expected if all of the Gd ions were participating in the ferromagnetic ordering. The entries in this table corresponding to γ = 5 mJ $mole^{-1}$ deg^{-2} are included to give some idea of the possible error introduced into this calculation by the assumption that γ is negligible. (Phillips and Matthias[49] came to the conclusion that $\gamma \approx 4$ mJ $mole^{-1}$ deg^{-2} on the basis of the size of the superconducting transition.) The entropy calculation was terminated at 18°K because the calculated lattice heat capacity and the observed heat capacity are equal at that temperature (see Figs. 14 and 15). Due to uncertainties in the derivation of the lattice heat capacity and to the assumption that γ is negligible, the resulting magnetic entropies could be in error by as much as 10%. Within this uncertainty of the entropy calculation, these results indicate that the entire volume of the sample participates in the ferromagnetic ordering. Even with a 10% uncertainty in the magnetic entropy the size of the

Table VII Magnetic Entropy of $Y_{1-x}Gd_xOs_2$ from 0 to 18°K

	S_{obs} (mJ mole^{-1}deg^{-1})	S_{calc} (mJ mole^{-1}deg^{-1})	$\frac{S_{obs}}{S_{calc}}$
γ=0[a]	817	690	1.18
X=0.04 γ=5	727	690	1.05
γ=0	1300	1300	1.00
X=0.075 γ=5	1210	1300	0.93

[a] The units of γ are mJ mole^{-1} deg^{-2}.

anomaly associated with the superconducting transition makes it very unlikely that superconductivity and ferromagnetism are not coexistent.

The heat capacity of the 4% Gd sample presents an interesting contrast to that of the 7.5% Gd sample. The results for the latter are roughly what one would expect for a superconducting transition taking place independently of and superposed on a magnetic ordering, i.e., a large, fairly regular magnetic ordering anomaly on which is superposed a smaller anomaly from the superconducting ordering. The heat capacity of the 4% Gd sample is different in two respects. First, the heat capacity from 0.8 to 3.4°K is approximately constant. Second, the superconducting transition introduces a large irregularity into the heat capacity curve. This irregularity, being essentially unaffected by magnetic fields of up to 300 Oe, is apparently largely associated with the magnetic ordering. This would indicate that the superconducting ordering of the conduction electrons, when taking place at temperatures at which the magnetic ordering is largely incomplete, significantly modifies the magnetic ordering process. That the two ordering processes should interact is not surprising since the magnetic ordering in these systems results from coupling of the 4f electrons of the Gd ions via interaction with the conduction electrons.

FIGURE CAPTIONS

Fig. 1 Schematic diagram of apparatus.

Fig. 2 Schematic diagram of ^3He pumping line.

Fig. 3 The heat capacity of ruthenium. The symbols ▲ and ■ denote two separate experiments. The superconducting-state heat capacity is extrapolated to 0°K on the basis of Eq. (5) of the text with a=8.12 and b=1.40.

Fig. 4 The heat capacity of ruthenium in the vicinity of the superconducting transition. The open and closed symbols denote two separate experiments.

Fig. 5 The superconducting-state electronic heat capacity of ruthenium. The symbols denote two separate experiments.

Fig. 6 The deviation of the reduced critical field of ruthenium from a parabola. $h=H_c/H_o$; $t=T/T_c$.

Fig. 7 Correlation of the quantities $V_m H_o^2/8\pi\gamma T_c^2$ and $2\epsilon(0)/kT_c$ vs T_c/Θ_o for several superconductors. The symbols ⊛ and △ represent independent measurements (see Table IV).

Fig. 8 The heat capacity of titanium: measurements in an adiabatic demagnetization cryostat.

Fig. 9 Partial phase diagram of the Ti-Fe alloy system. The dashed line represents the martensitic start temperature. For detailed discussion of the Ti-Fe phase diagram, see Ref. 35.

Fig. 10 The heat capacity of $Ti_{0.9995}Fe_{0.0005}$.

Fig. 11 The heat capacity of $Ti_{0.9975}Fe_{0.0025}$ measured in zero magnetic field. The two symbols denote separate experiments.

Fig. 12 The heat capacity of $Ti_{0.99}Fe_{0.01}$ measured in zero magnetic field. The dashed line represents the electronic and lattice heat capacity measured at $T < 1°K$ (see Fig. 13). The use of A as the coefficient of the T^3 term in the equation for the solid line implies that the slope of this line is not representative of the lattice heat capacity of the sample (see text).

Fig. 13 The heat capacity of $Ti_{0.99}Fe_{0.01}$ in zero magnetic field at $T < 1°K$. The ○ represents measurements in the ^3He calorimeter; the △ represents measurements in an adiabatic-demagnetization calorimeter.

Fig. 14 The heat capacity of $Y_{0.96}Gd_{0.04}Os_2$. T_c and T_s are, respectively, the ferromagnetic Curie point and superconducting transition temperature obtained by magnetic measurements. The unlabled arrows designate temperatures at which the heat capacity curves measured in H=0 and 300 Oe cross.

Fig. 15 The heat capacity of $Y_{0.925}Gd_{0.075}Os_2$. T_s and T_c have the same significance as in Fig. 14.

Fig. 16 The heat capacity of $Y_{0.925}Gd_{0.075}Os_2$ in the vicinity of the superconducting transition.

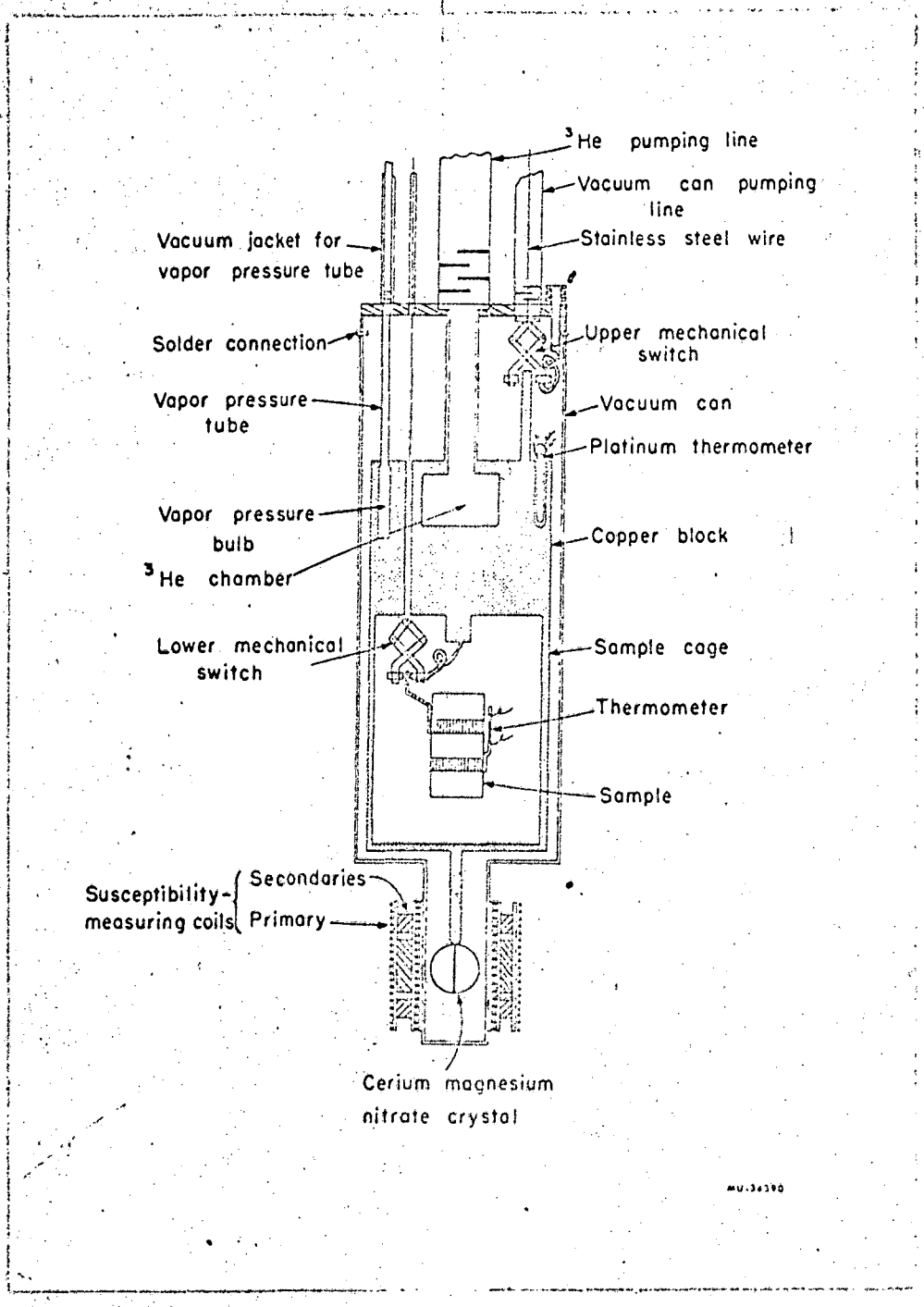
^{3}He pumping line
Vacuum can pumping line
Stainless steel wire
Vacuum jacket for vapor pressure tube
Solder connection
Upper mechanical switch
Vapor pressure tube
Vacuum can
Platinum thermometer
Vapor pressure bulb
^{3}He chamber
Copper block
Lower mechanical switch
Sample cage
Thermometer
Sample
Susceptibility-measuring coils
Secondaries
Primary
Cerium magnesium nitrate crystal

Figure 1

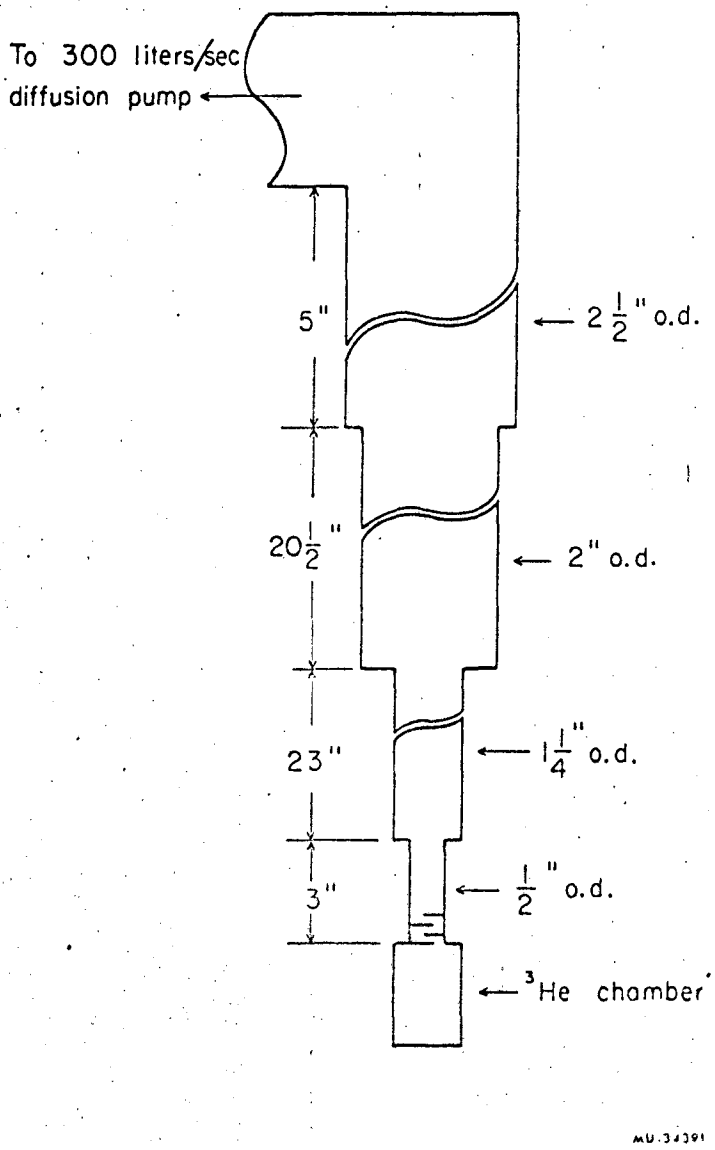
To 300 liters/sec
diffusion pump
5"
2 1/2" o.d.
20 1/2"
2" o.d.
23"
1 1/4" o.d.
3"
1/2" o.d.
3He chamber
MU-34391

Figure 2

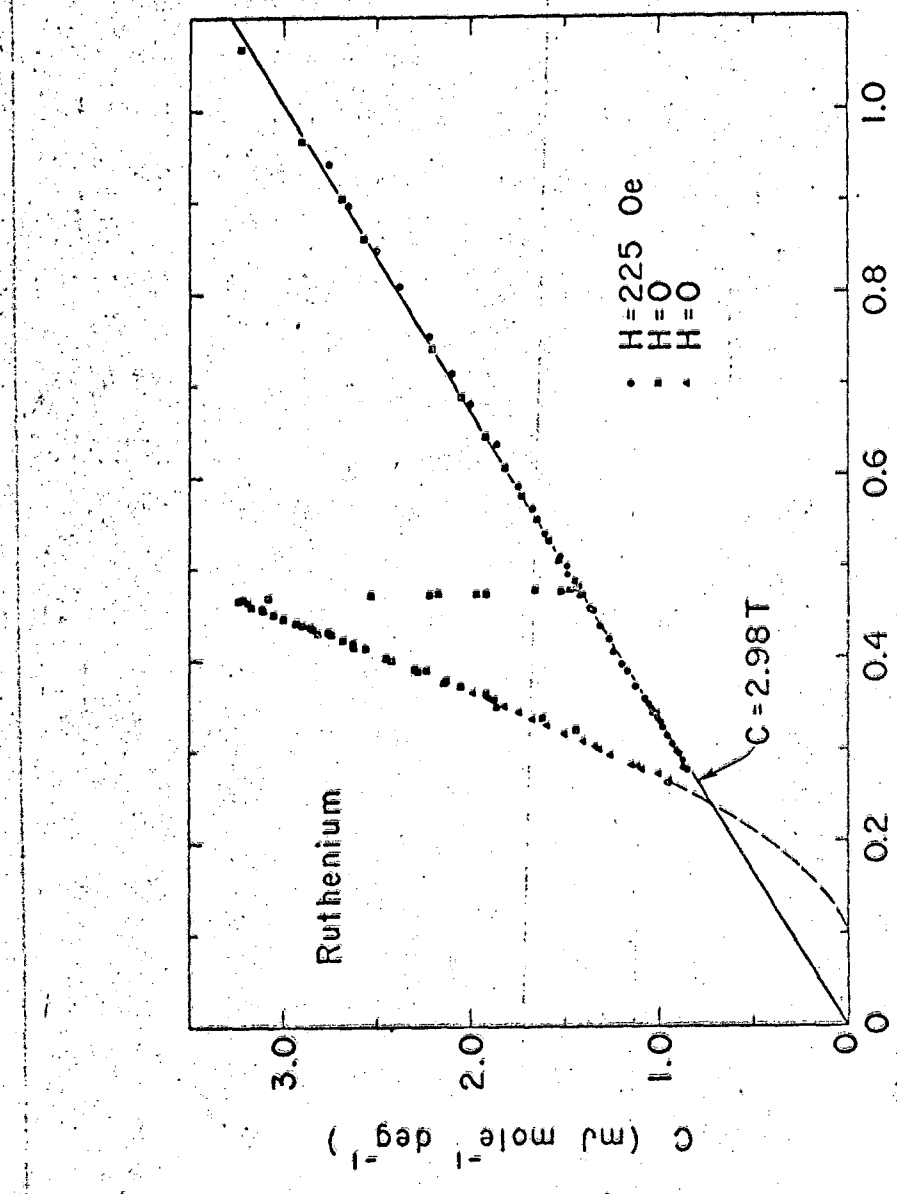
Ruthenium
H=225 Oe
H=0
H=0
C=2.98T
T (°K)
C (mJ mole⁻¹ deg⁻¹)
0
0.2
0.4
0.6
0.8
1.0
1.0
2.0
3.0

Figure 3

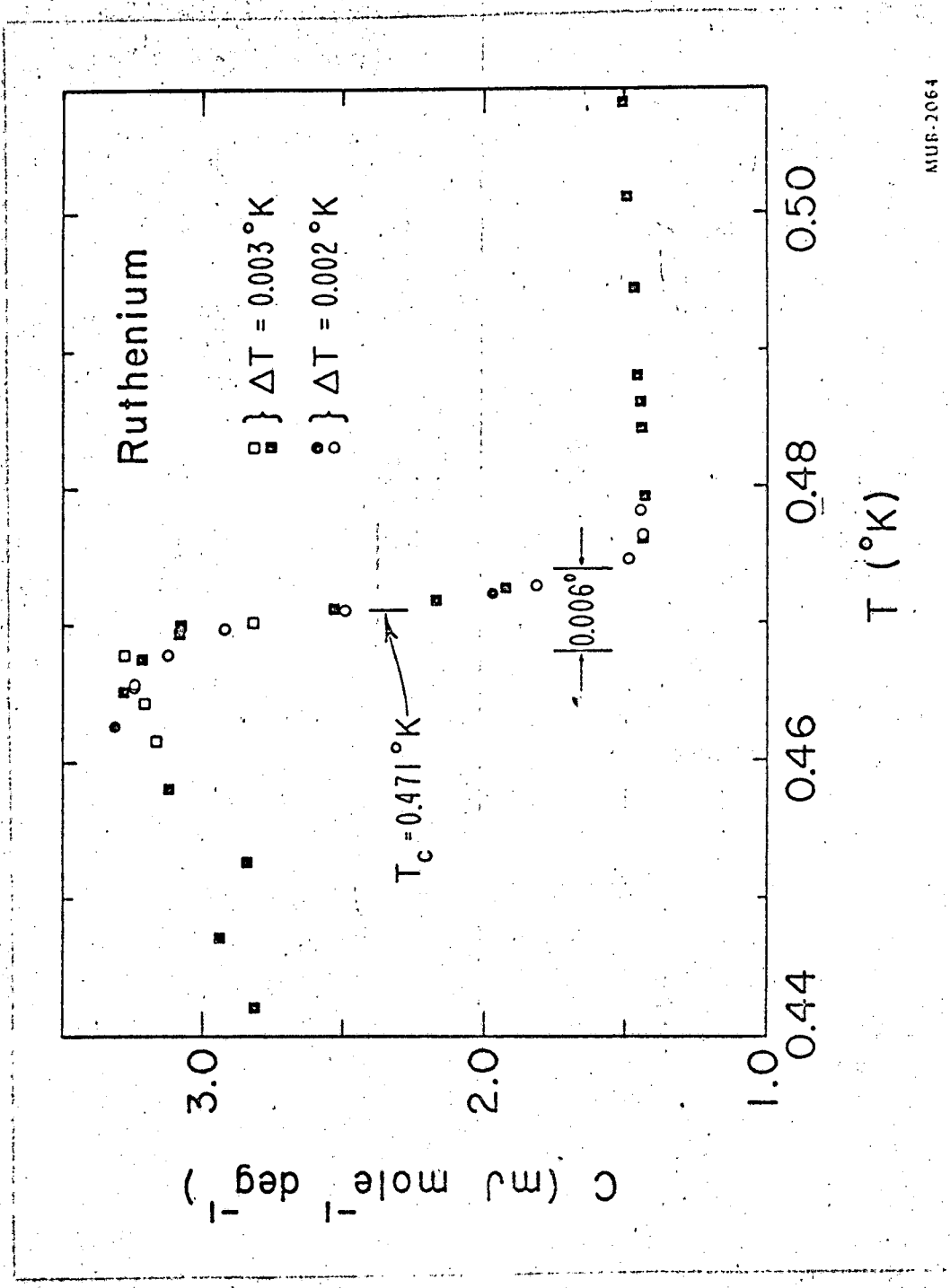
Ruthenium
} ΔT = 0.003°K
} ΔT = 0.002°K
T_c = 0.471°K
0.006°
C (mJ mole^{-1} deg^{-1})
3.0
2.0
1.0
0.44
0.46
0.48
0.50
T (°K)
MUB-2064

Figure 4

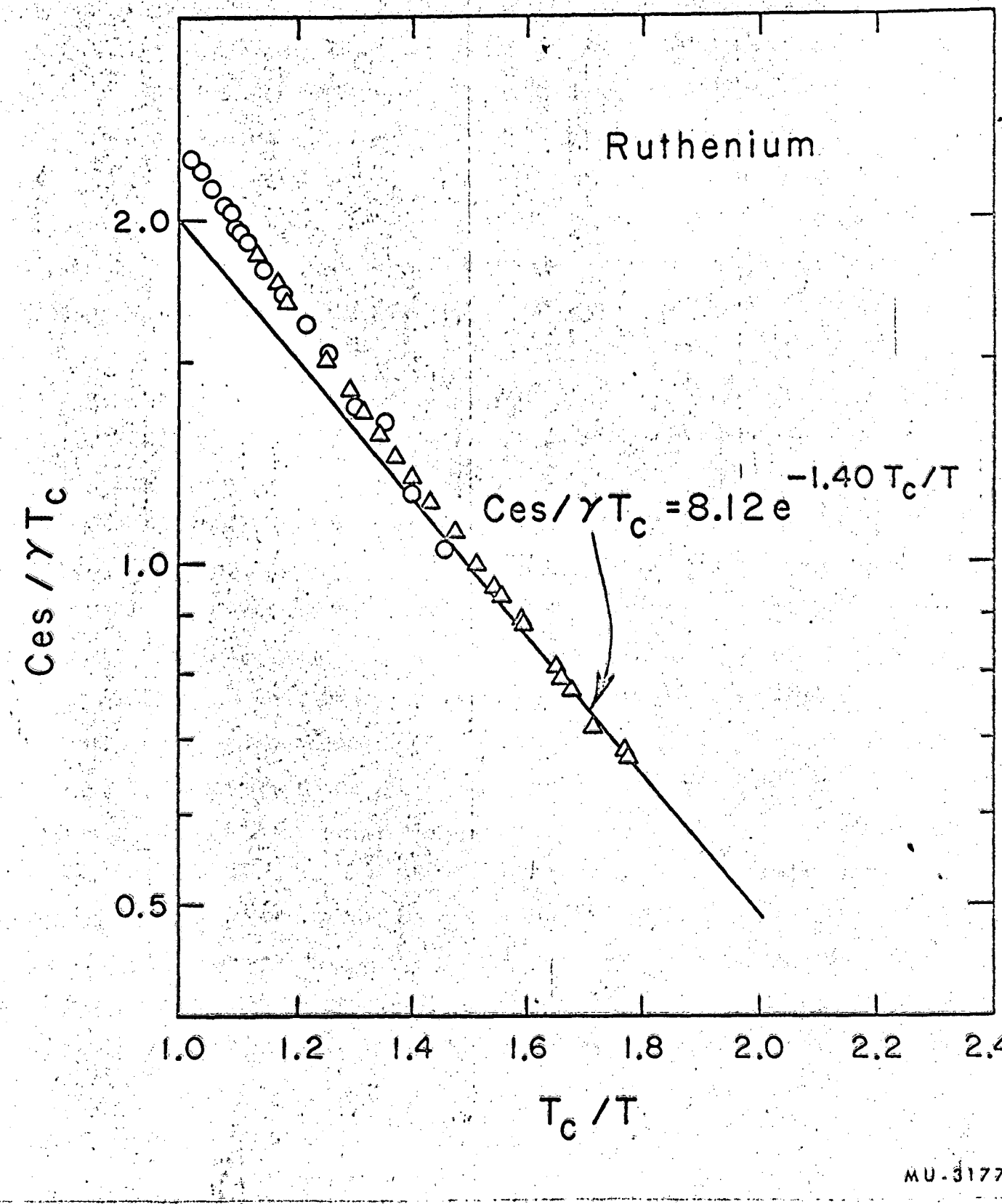
Ruthenium
$Ces/\gamma T_c = 8.12\, e^{-1.40\, T_c/T}$
$Ces/\gamma T_c$
T_c/T
2.0
1.0
0.5
1.0
1.2
1.4
1.6
1.8
2.0
2.2
2.4
MU-31771

Figure 5

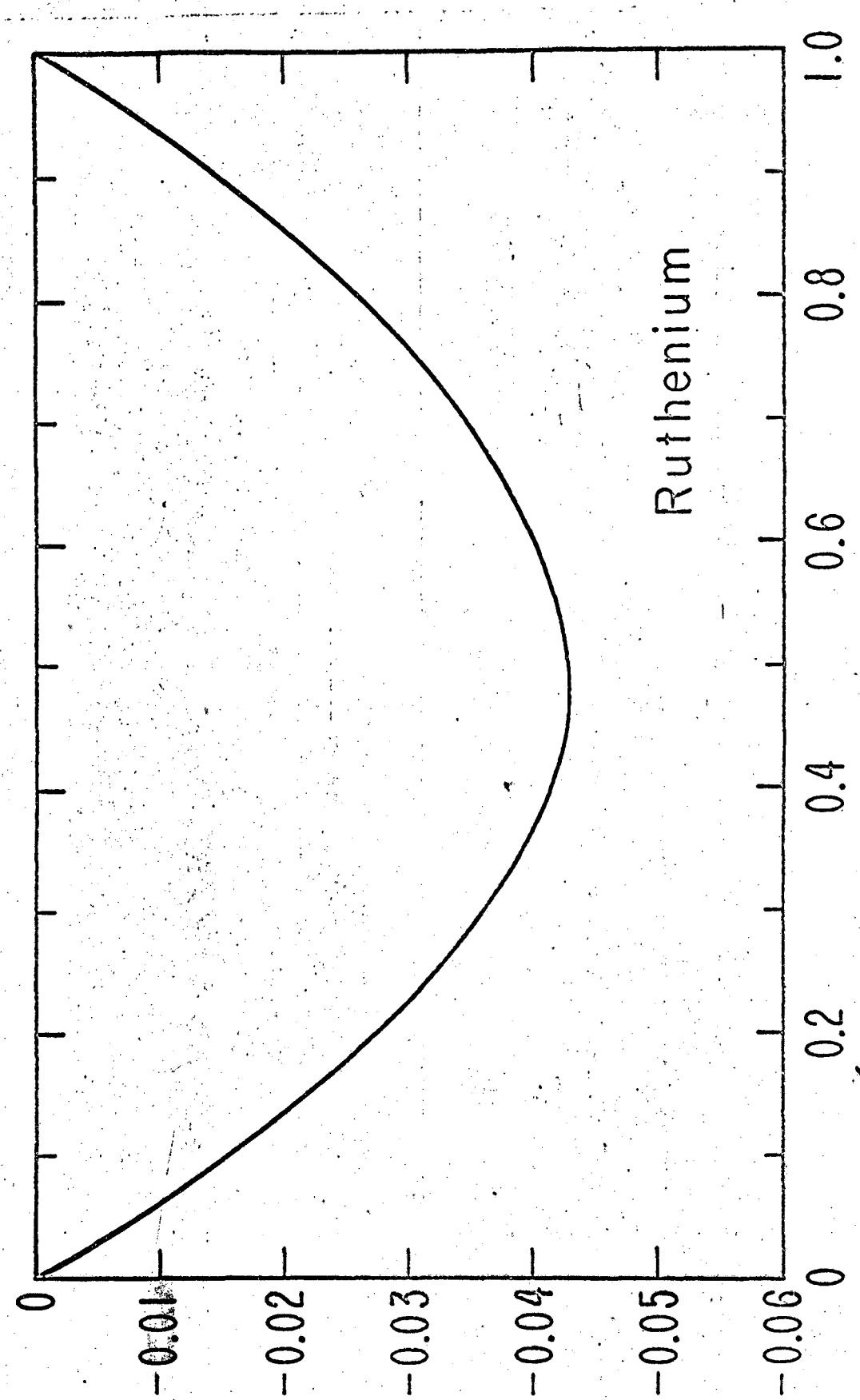

Figure 6

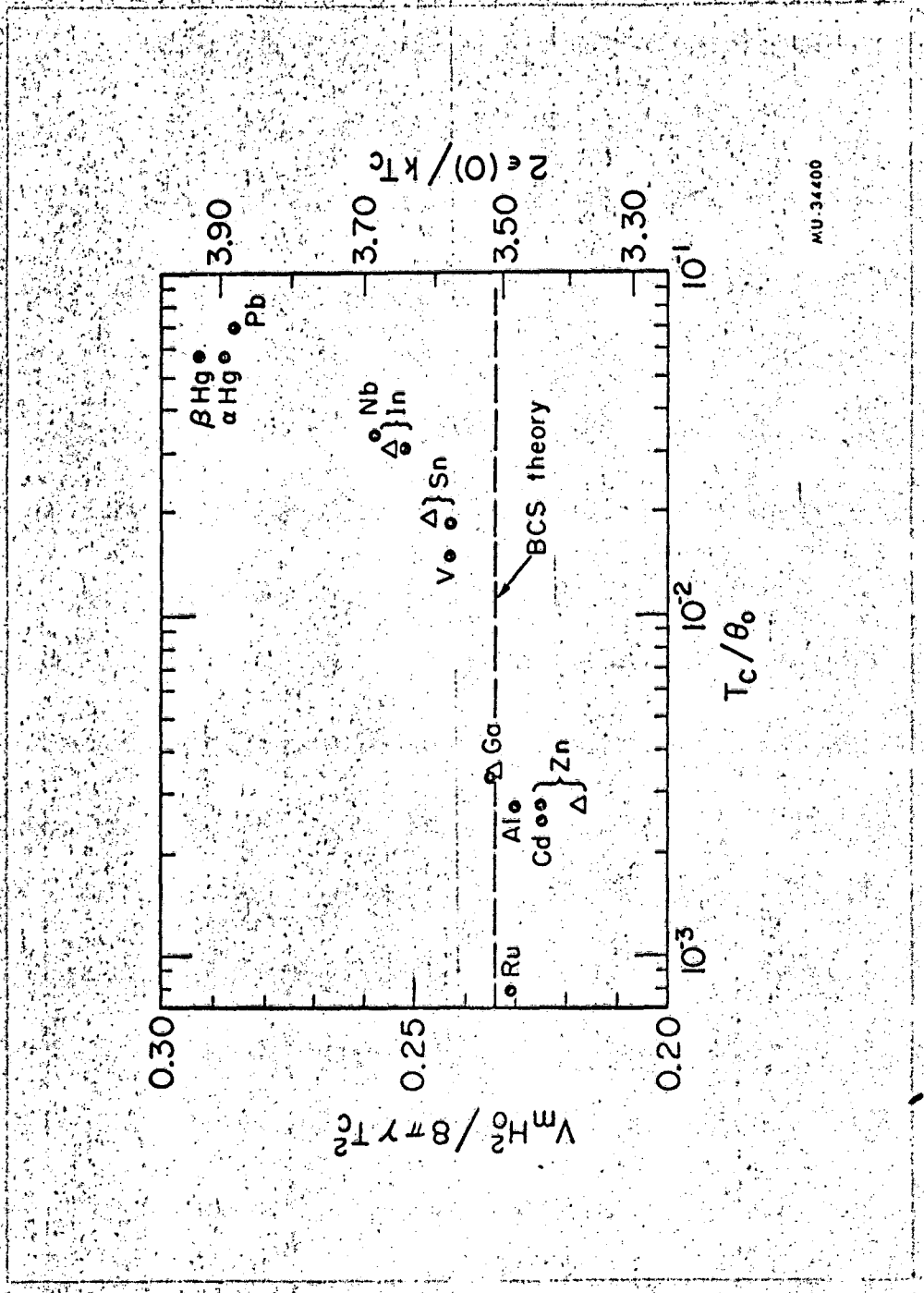
MU-34400
$N_e(0)/kT_c$
3.90
3.70
3.50
3.30
10^{-1}
10^{-2}
10^{-3}
T_c/θ_o
$V_m H_o^2/8\pi\gamma T_c^2$
0.30
0.25
0.20
βHg
αHg
Pb
Nb
In
V
Sn
BCS theory
Ga
Al
Cd
Zn
Ru

Figure 7

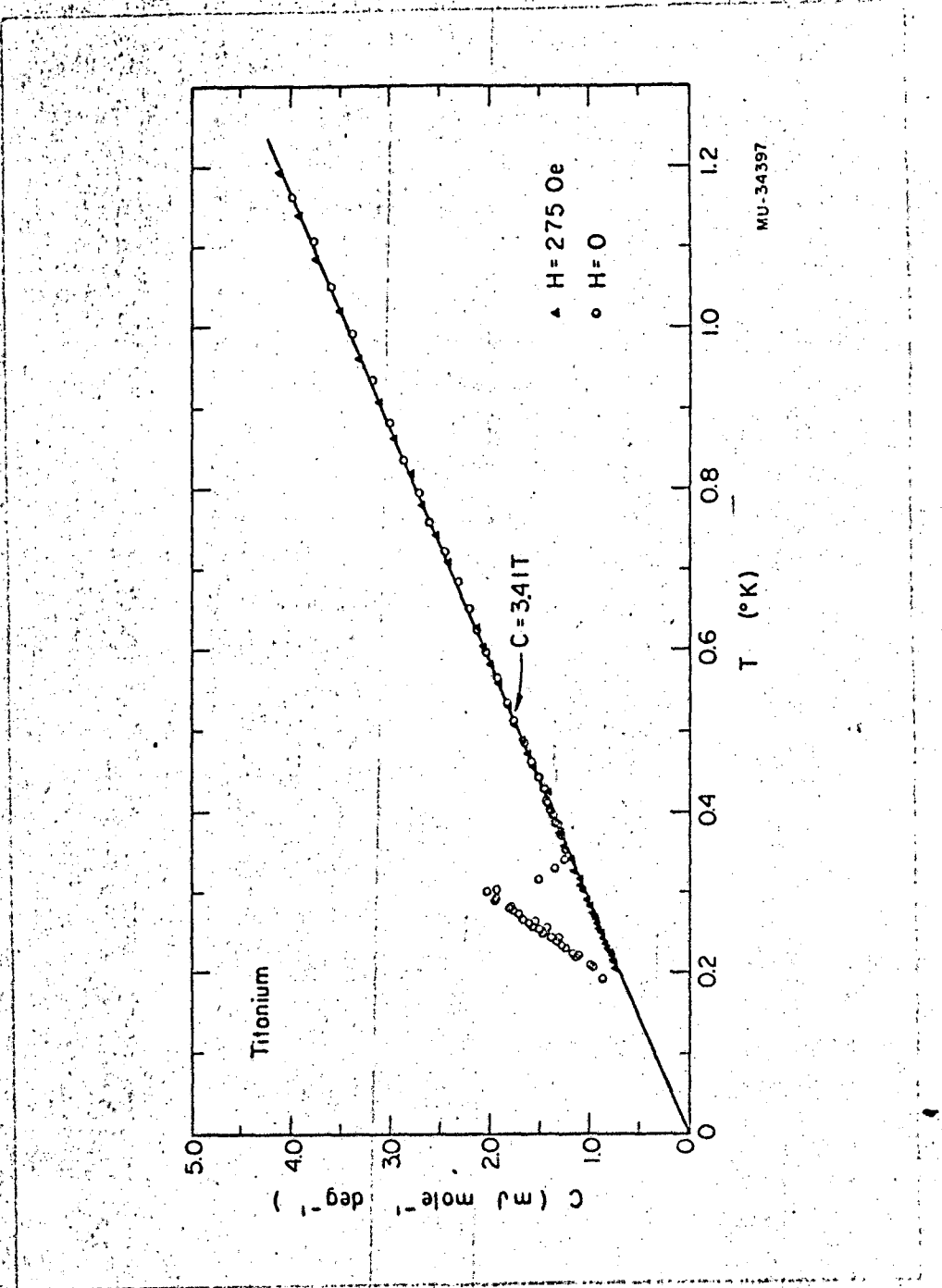
Titanium
C = 3.41T
H = 275 Oe
H = 0
MU-34397
C (mJ mole⁻¹ deg⁻¹)
T (°K)
0
1.0
2.0
3.0
4.0
5.0
0.2
0.4
0.6
0.8
1.0
1.2

Figure 8

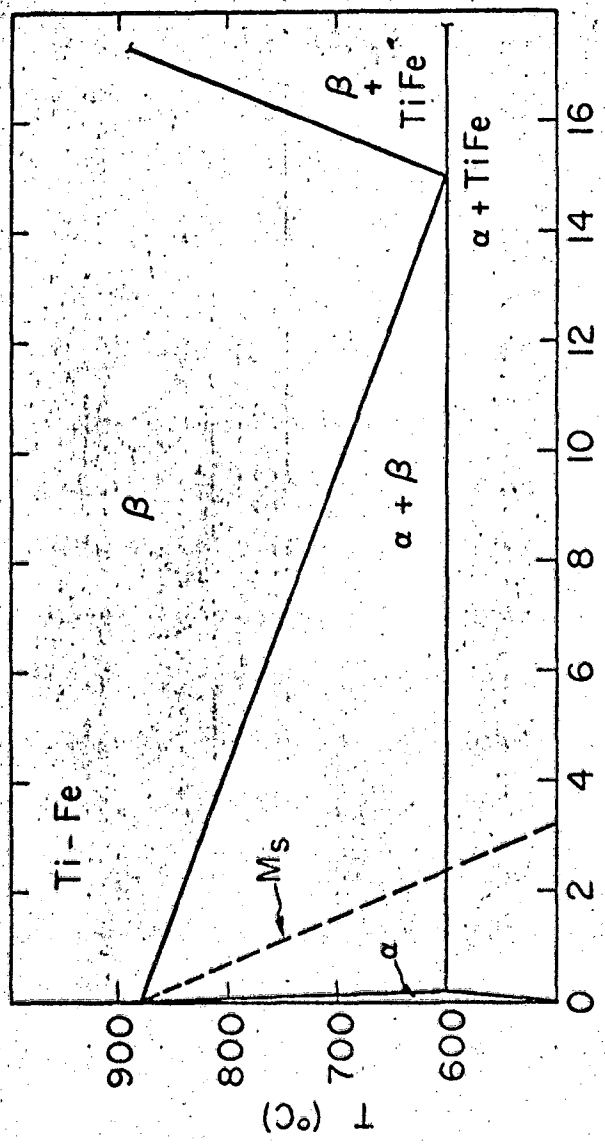
MU-34399
β
β + TiFe
α + TiFe
α + β
Ti - Fe
Ms
α
T (°C)
900
800
700
600
0
2
4
6
8
10
12
14
16
Wt % Fe

Figure 9

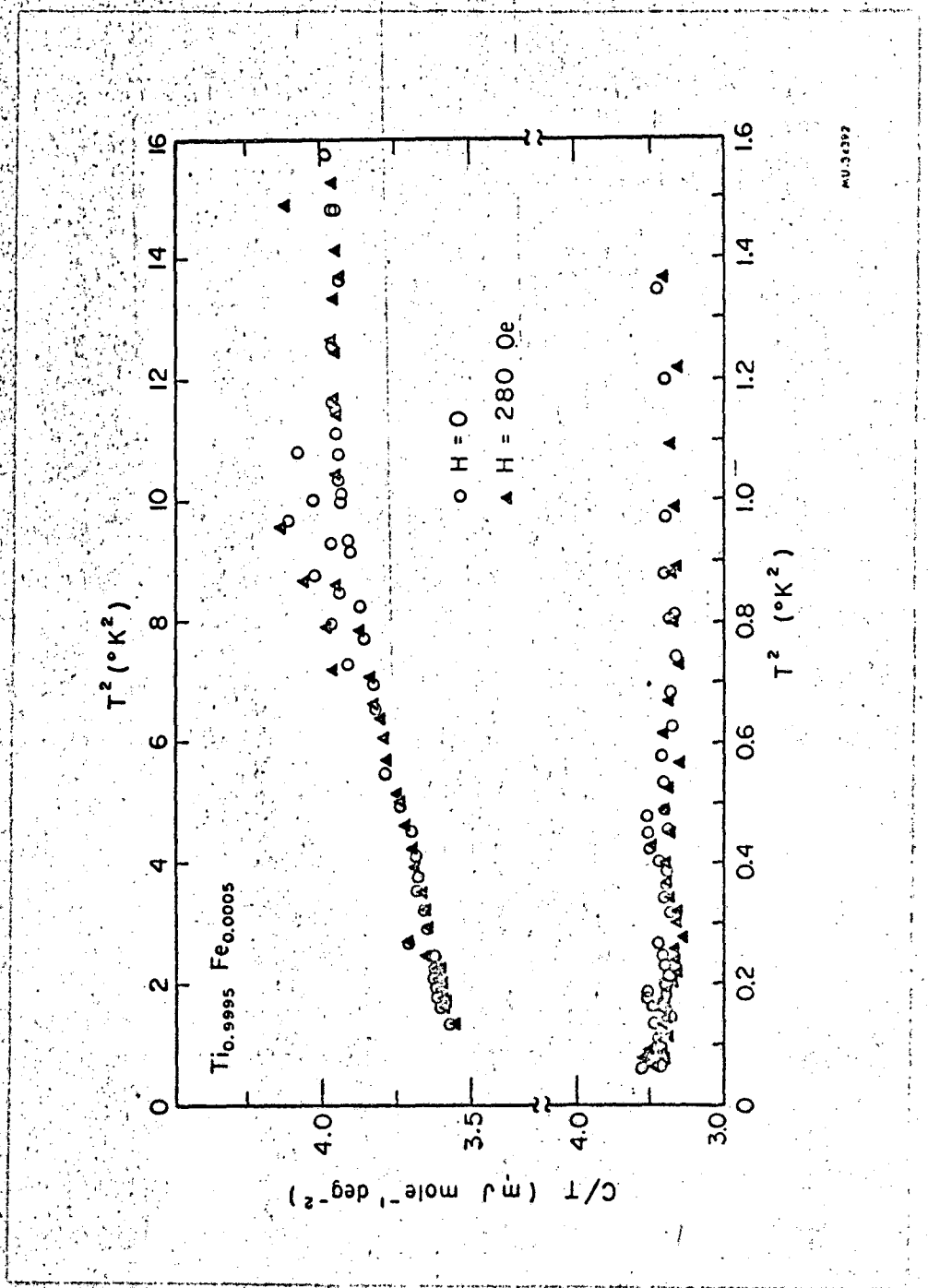
$Ti_{0.9995}$ $Fe_{0.0005}$
o H = 0
▲ H = 280 Oe
T^2 (°K²)
T^2 (°K²)
C/T (mJ mole⁻¹ deg⁻²)
MU-34392

Figure 10

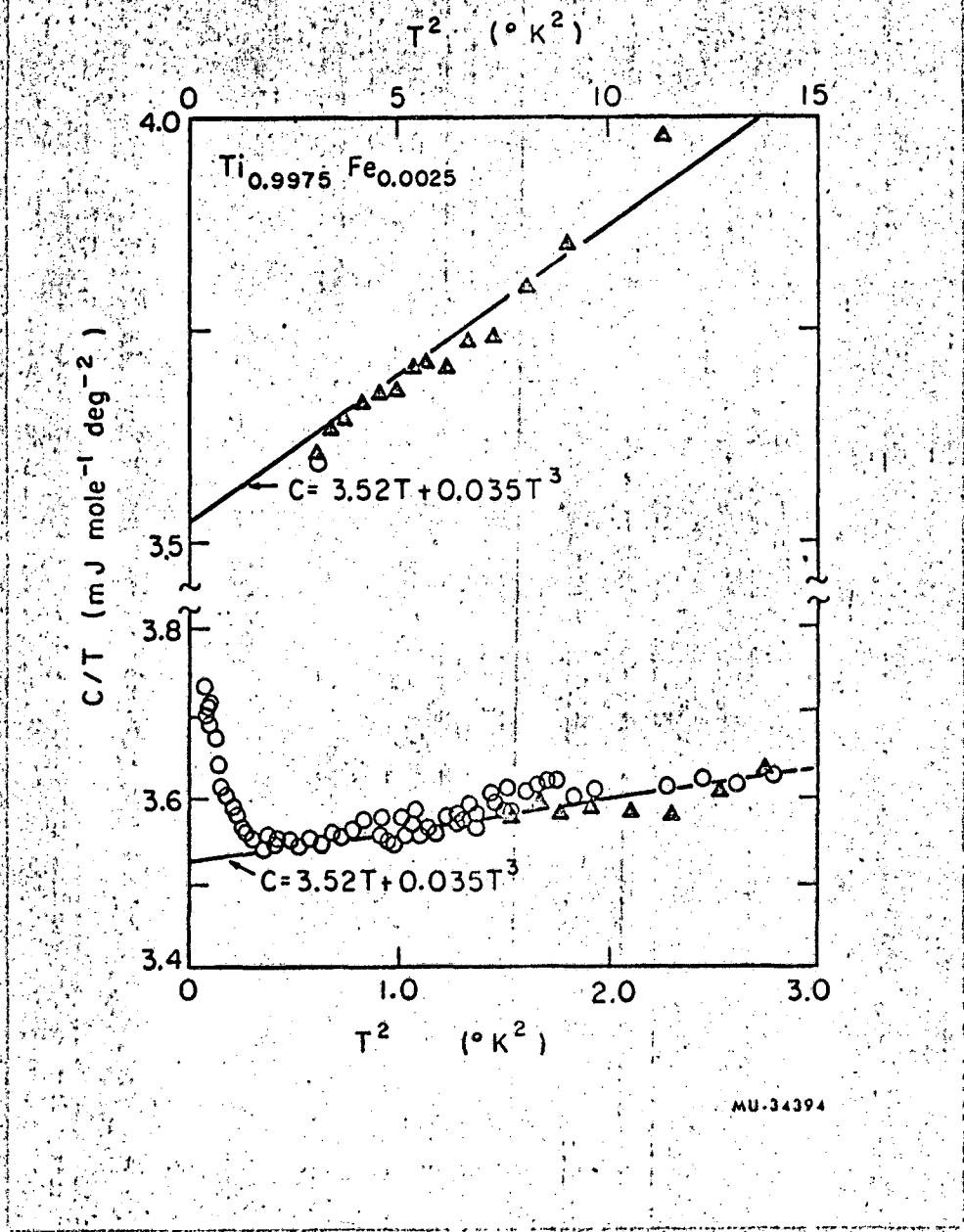
T^2 (°K^2)
0
5
10
15
4.0
$Ti_{0.9975}$ $Fe_{0.0025}$
C= 3.52T + 0.035T^3
3.5
3.8
3.6
C= 3.52T + 0.035T^3
3.4
C/T (mJ mole^{-1} deg^{-2})
0
1.0
2.0
3.0
T^2 (°K^2)
MU-34394

Figure 11

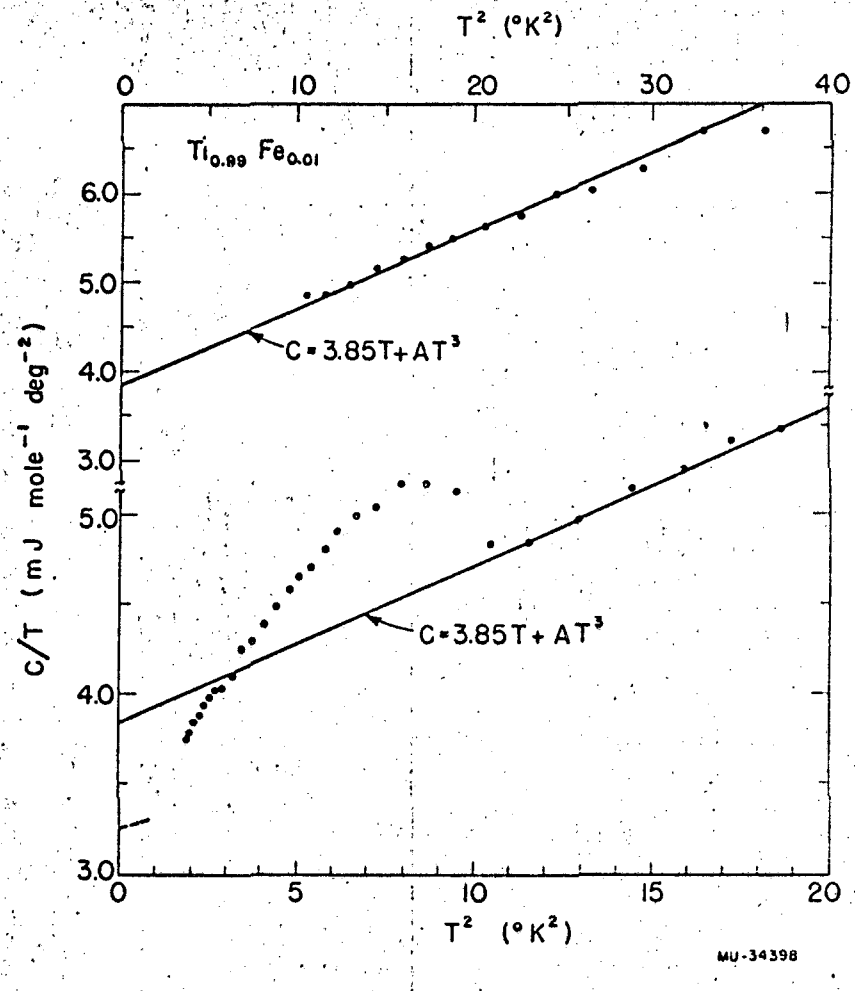
T² (°K²)
0
10
20
30
40
Ti0.99 Fe0.01
6.0
5.0
4.0
3.0
C = 3.85T + AT³
C = 3.85T + AT³
C/T (mJ mole⁻¹ deg⁻²)
5.0
4.0
3.0
0
5
10
15
20
T² (°K²)
MU-34398

Figure 12

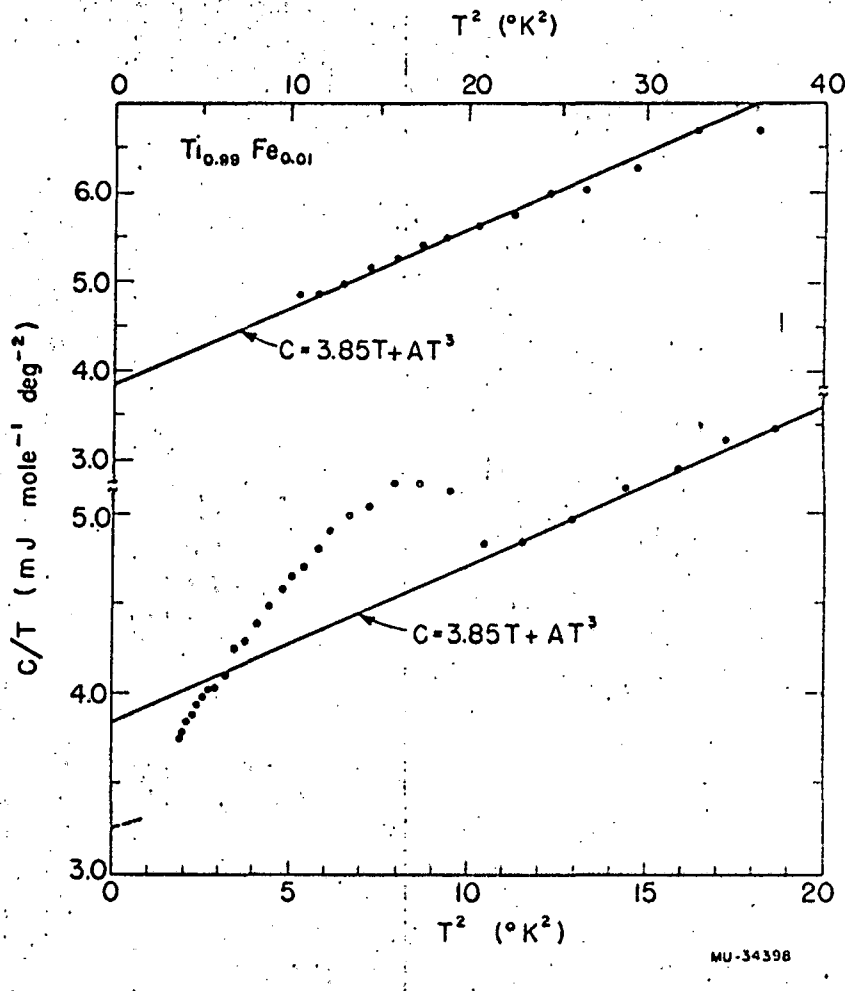
T² (°K²)
0
10
20
30
40
Ti0.99 Fe0.01
6.0
5.0
4.0
3.0
C = 3.85T + AT³
C/T (mJ mole⁻¹ deg⁻²)
5.0
4.0
3.0
C = 3.85T + AT³
0
5
10
15
20
T² (°K²)
MU-34398

Figure 12

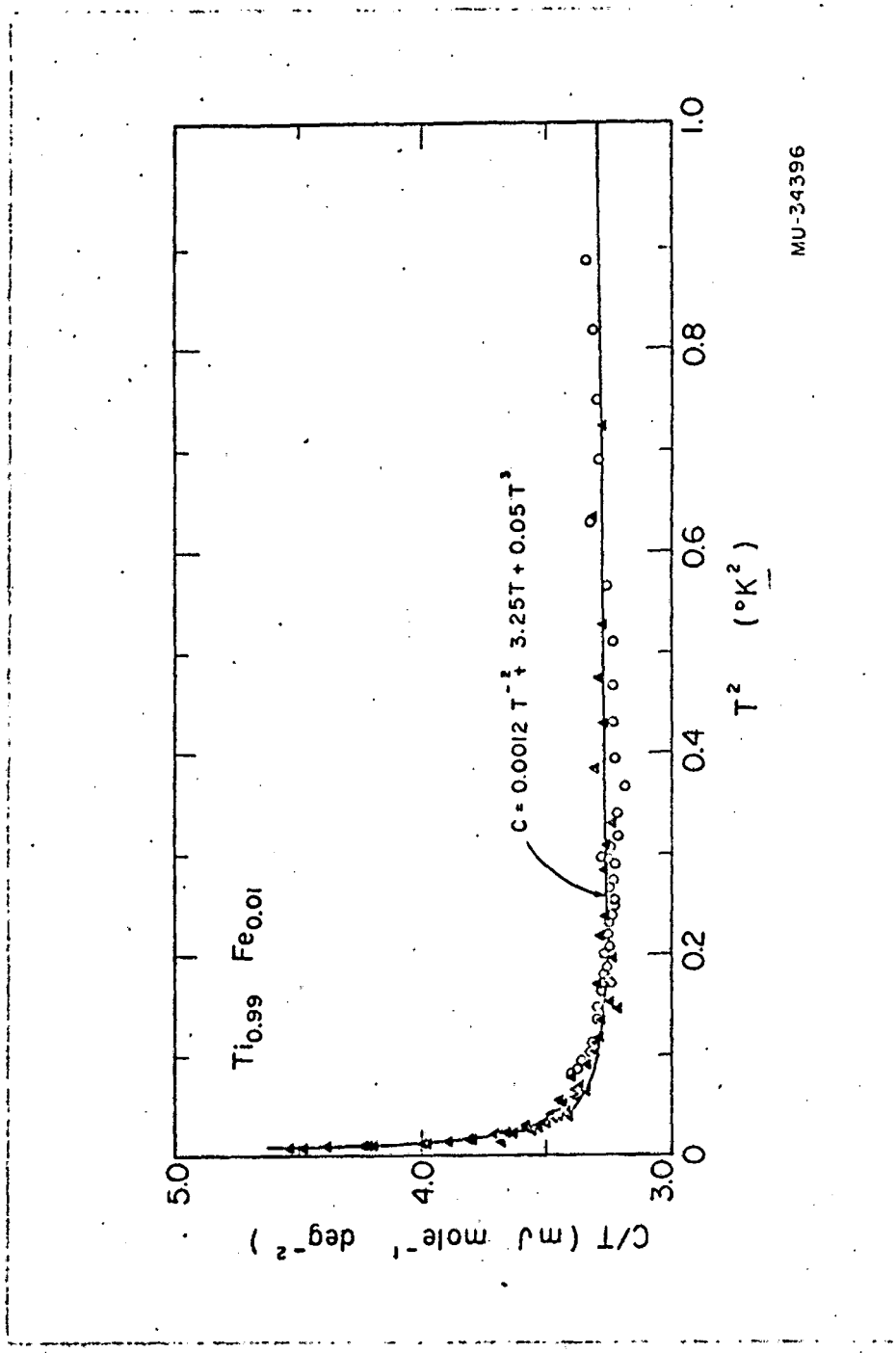
MU-34396
C/T (mJ mole⁻¹ deg⁻²)
T² (°K²)
Ti0.99 Fe0.01
C = 0.0012 T⁻³ + 3.25T + 0.05T³
5.0
4.0
3.0
0
0.2
0.4
0.6
0.8
1.0

Figure 13

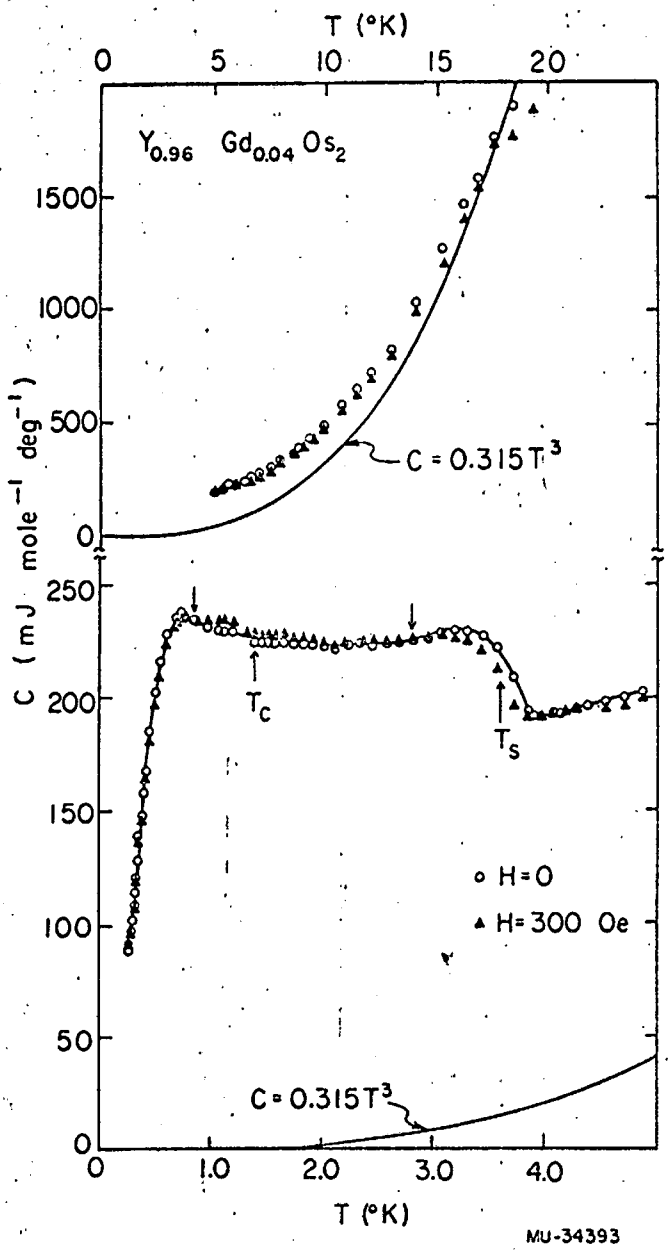
T (°K)
0
5
10
15
20
$Y_{0.96}$ $Gd_{0.04}$ Os_2
1500
1000
500
0
$C = 0.315T^3$
C (mJ mole^{-1} deg^{-1})
250
200
150
100
50
0
T_c
T_s
o H=0
▲ H=300 Oe
$C = 0.315T^3$
0
1.0
2.0
3.0
4.0
T (°K)
MU-34393

Figure 14

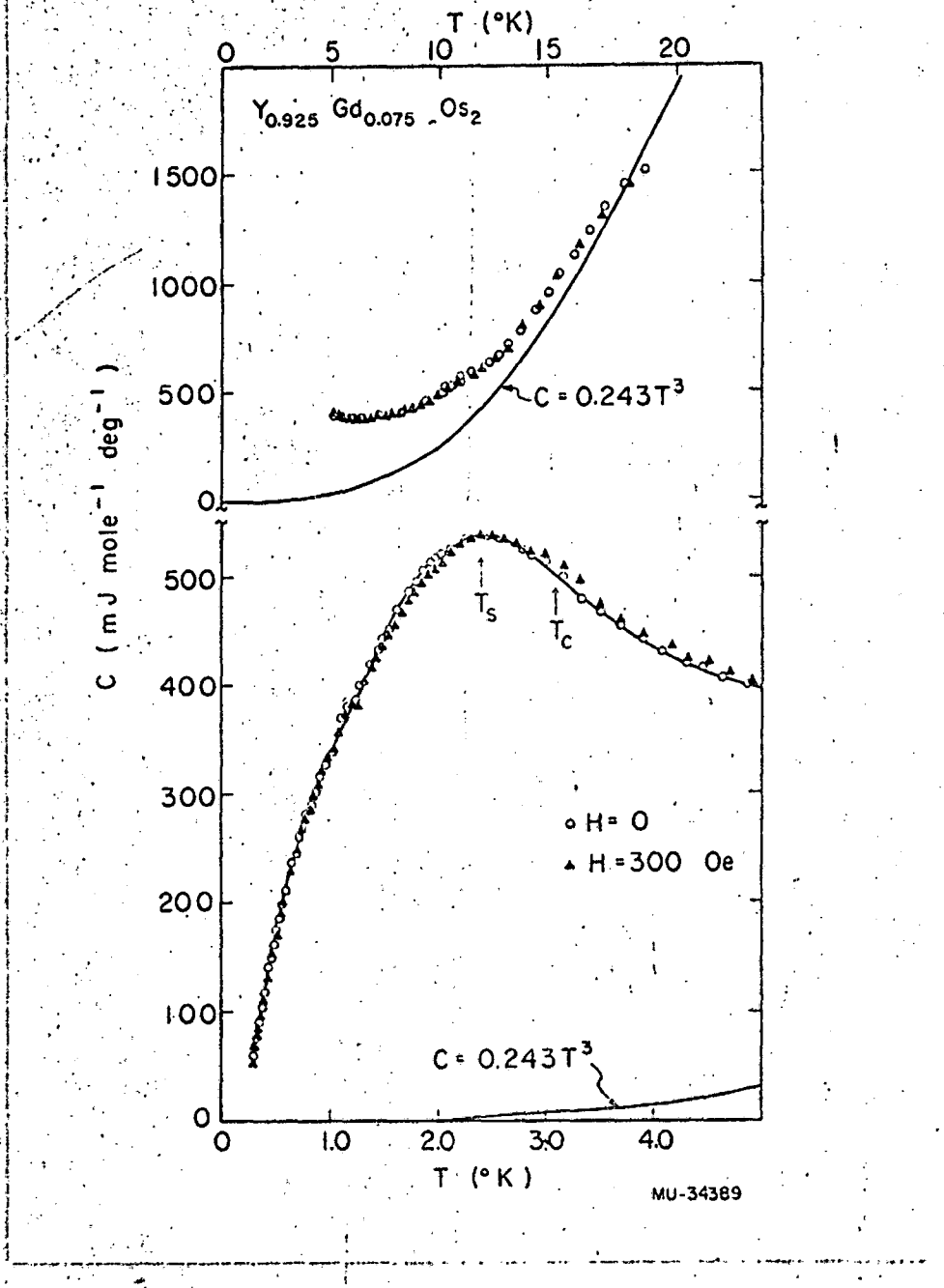
T (°K)
0
5
10
15
20
$Y_{0.925}$ $Gd_{0.075}$ Os_2
1500
1000
500
0
C = 0.243T³
C (mJ mole⁻¹ deg⁻¹)
500
400
300
200
100
0
T_S
T_C
o H= 0
▲ H=300 Oe
C = 0.243T³
0
1.0
2.0
3.0
4.0
T (°K)
MU-34389

Figure 15

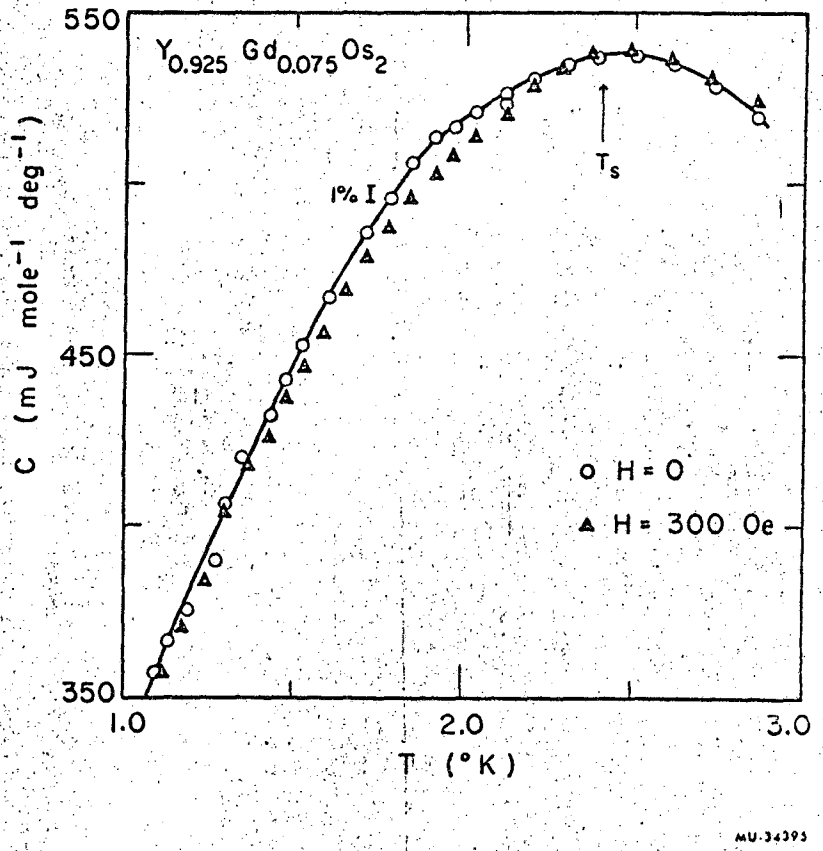
550
450
350
1.0
2.0
3.0
$Y_{0.925}\ Gd_{0.075}Os_2$
1% I
T_s
o H = 0
▲ H = 300 Oe
C (mJ mole^{-1} deg^{-1})
T (°K)
MU-34395

Figure 16

ACKNOWLEDGMENTS

The author wishes to thank the following persons: Dr. T. H. Geballe of Bell Telephone Laboratories for supplying the samples used in these experiments and for several helpful discussions; Mrs. Patricia Cookson for her expeditious typing and editing of this thesis; and Professor Norman E. Phillips, under whose inspiring guidance this work was carried out.

This work was performed under the auspices of the United States Atomic Energy Commission and the National Science Foundation.

REFERENCES

1. E. J. Walker, Rev. Sci. Instr., 30, 834 (1959).
2. H. S. Sommers, Jr., Rev. Sci. Instr., 25, 793 (1954).
3. H. N. Wooley, R. B. Scott and F. G. Brickwedde, J. Res. Natl. Bur. Standards, 41, 379 (1948) PR 1932.
4. The 1958 He^4 Scale of Temperatures, NBS Monograph 10, (U.S. Department of Commerce, National Bureau of Standards, Washington 25, D.C. June 17, 1960).
5. G. Cataland, M. H. Edlow and H. H. Plumb in Temperature, C. M. Herzfeld (Ed.)(Reinhold Publishing Company, New York, 1962), Vol. III, Part 1, p. 413.
6. J. M. Daniels and F. N. K. Robinson, Phil. Mag., 44, 630 (1953).
7. R. A. Erickson, L. D. Roberts and J. W. T. Dabbs, Rev. Sci. Instr., 25, 1178 (1954).
8. R. B. Scott, G. A. Kilgore and R. E. Gaumer in National Bureau of Standards Report #2 for Office of Naval Research Contract NAonr 12-48 for Low Temperature Research at the National Bureau of Standards, (US Department of Commerce, National Bureau of Standards, Washington 25, D.C.), p. 21.
9. N. E. Phillips, Phys. Rev. 134, A385 (1964).
10. H. R. O'Neal and N. E. Phillips (to be published).
11. N. E. Phillips, Phys. Rev., 114, 676 (1959).
12. E. Maxwell, Phys. Rev., 78, 477 (1950).
13. C. A. Reynolds, B. Serin, W. H. Wright and L. B. Nesbitt, Phys. Rev., 78, 487 (1950).
14. E. Maxwell, Phys. Rev., 86, 235 (1952).

15. W. D. Allen, R. H. Dawton, J. M. Lock, A. B. Pippard and D. Shoenberg, Nature, London, 166, 1071 (1950).

16. E. Maxwell, Natl. Bur. Standards Circ., 519, 29 (1952).

17. M. Olsen-Bär, Nature (London), 168, 245 (1951).

18. H. R. O'Neal, N. M. Senozan and N. E. Phillips, Proceedings of the Eighth International Conference on Low-Temperature Physics, London, 1962, (Butterworths Scientific Publications, Ltd., London, 1962).

19. T. H. Geballe and B. T. Matthias, IBM J. Research Develop. 6, 256 (1962).

20. J. L. Olsen, Cryogenics, 2, 356 (1962).

21. H. Frohlich, Phys. Rev., 79, 845 (1950).

22. T. H. Geballe, B. T. Matthias, G. W. Hull, Jr., and E. Corenzwit, Phys. Rev. Letters 6, 275 (1961).

23. D. K. Finnemore and D. E. Mapother, Phys. Rev. Letters, 9, 288 (1962).

24. R. A. Hein and J. W. Gibson, Phys. Rev., 131, 1105 (1963).

25. B. T. Matthias, T. H. Geballe, E. Corenzwit and G. W. Hull, Jr., Phys. Rev., 129, 1025 (1963).

26. J. W. Garland, Phys. Rev. Letters, 11, 111 (1963).

27. J. C. Swihart, IBM J. Research Develop., 6, 14 (1962).

28. P. Morel and P. W. Anderson, Phys. Rev., 125, 1263 (1962).

29. Rare Metals Handbook, Second Edition, C. A. Hampel (Ed.), (Reinhold Publishing Company, London, 1961), p. 324.

30. B. B. Goodman, Compt. rend., 246, 3031 (1958).

31. B. T. Matthias, H. Suhl and E. Corenzwit, Phys. Rev. Letters, 1, 92 (1958).

32. B. T. Matthias, V. B. Compton, H. Suhl and E. Corenzwit, Phys. Rev., 115, 1597 (1959).

33. T. H. Geballe, Revs. Mod. Phys., 36, (Part 1), 134 (1964).

34. R. L. Falge, Jr., Phys. Rev. Letters, 11, 248 (1963).

35. The following discussion, as well as Fig. 9, is based on information drawn from the following two sources: Constitution of Binary Alloys, M. Hansen, (McGraw-Hill Book Company, Inc., New York, 1958) and Titanium, A. D. McQuillan and M. K. McQuillan (Butterworths Scientific Publications, London, 1956).

36. G. O. Arrhenius (private communication).

37. J. A. Cape, Phys. Rev., 132, 1486 (1963).

38. See Ref. i of Table V.

39. R. R. Hake, D. H. Leslie, and T. G. Berlincourt, Phys. Rev., 127, 170 (1962).

40. N. E. Phillips (unpublished).

41. A. A. Abrikosov and L. P. Gorkov, Zh. Esperim. i Teor. Fiz., 39, 1781 (1960) [English Trans. Soviet Phys.-JETP, 12, 1243 (1961)].

42. F. Heiniger and J. Muller, Phys. Rev., 134, A1407 (1964).

43. B. T. Matthias, H. Suhl and E. Corenzwit, Phys. Rev. Letters, 1, 92 (1958).

44. R. A. Hein, F. L. Falge, Jr., B. T. Matthias and E. Corenzwit, Phys. Rev. Letters, 2, 500 (1959).

45. B. T. Matthias, H. Suhl and E. Corenzwit, Phys. Rev. Letters, 1, 449 (1958).

46. R. M. Bozorth, D. D. Davis and A. J. Williams, Phys. Rev., 119, 1570 (1960).

47. R. M. Bozorth, B. T. Matthias and D. D. Davis, Proceedings of the VIIth International Conference on Low Temperature Physics, 1960, G. M. Grahm and A. C. Hollis Hallet (Ed.), (University of Toronto

Press, Toronto, 1961), p. 385.

48. H. Suhl, B. T. Matthias and E. Corenzwit, J. Phys. Chem. Solids, 11, 346 (1959).

49. N. E. Phillips and B. T. Matthias, Phys. Rev., 121, 105 (1961).